Heat stress affects the cytoskeleton and the delivery of sucrose synthase in tobacco pollen tubes

Heat stress affects the cytoskeleton and the delivery of sucrose synthase in tobacco pollen tubes

Luigi Parrotta, Claudia Faleri, Mauro Cresti & Giampiero Cai

Dipartimento Scienze della Vita, Università di Siena, via Mattioli 4, 53100 Siena (Italy)

ABSTRACT

Abstract
Main conclusion Heat stress changes isoform content and distribution of cytoskeletal subunits in pollen tubes affecting accumulation of secretory vesicles and distribution of sucrose synthase, an enzyme involved in cell wall synthesis.
Plants are sessile organisms and are therefore exposed to damages caused by the predictable increase in temperature. We have analyzed the effects of temperatures on the development of pollen tubes by focusing on the cytoskeleton and related processes, such as vesicular transport and cell wall synthesis. First, we show that heat stress affects pollen germination and, to a lesser extent, pollen tube growth. Both, microtubules and actin filaments, are damaged by heat treatment and changes of actin and tubulin isoforms were observed in both cases. Damages to actin filaments mainly concern the actin array present in the subapex, a region critical for determining organelle and vesicle content in the pollen tube apex. In support of this, green fluorescent protein-labeled vesicles are arranged differently between heat-stressed and control samples. In addition, newly secreted cell wall material (labeled by propidium iodide) shows an altered distribution. Damage induced by heat stress also extends to proteins that bind actin and participate in cell wall synthesis, such as sucrose synthase. Ultimately, heat stress affects the cytoskeleton thereby causing alterations in the process of vesicular transport and cell wall deposition.

Keywords: heat stress; cytoskeleton; pollen tube; actin isoforms; cell wall

INTRODUCTION

Climate changes represent important challenges that all life forms will face in the next years (Bellard et al. 2012). The average temperature on Earth likely increased during the twentieth century and temperatures are expected to rise more by the end of the twenty-first century. As plants are sessile organisms, they are constantly exposed to temperature variations; therefore, they have developed a series of responses that minimize damage and maintain the cellular homeostasis. Although some positive effects are expected from the increase of temperatures, it is likely that climate variations will cause a decrease in crop yield and will affect agriculture because of shorter life cycles and acceleration of senescence (Porter 2005). The increase of temperatures is likely to have negative effects on several aspects of plants, from root elongation to plant growth, from leaf development to reproduction (Wahid et al. 2007). Damage caused by high temperatures to reproductive organs may potentially threaten plant survival. Both the female and male reproductive organs are sensitive to changes of temperature (Zinn et al. 2010) with male organs being more vulnerable to thermal stress (Sato et al. 2006). Pollen formation is a developmental stage highly sensitive to temperature fluctuation in cereals (Prasad et al. 2008) as well as in wheat (Wollenweber et al. 2003). In the latter, abortion of tapetum cells, which hinders microspores to complete the first mitotic division, results in the absence of maturation. Although microspores might eventually complete the first mitotic division, only few of them can further divide and develop into the characteristic tricellular pollen grain; the rest of microspores remain immature and do not accumulate starch (Saini et al. 1983). Heat stress ([30

———————————C) from the onset of meiosis to pollen maturation has also a detrimental effect on the viability of pollen grains in wheat, with consequent decrease in fertilization and seed production (Saini and Aspinall 1982). In Cicer arietinum L., heat stress caused reduction of pod set by affecting pollen viability and pollen production and therefore seed number (Devasirvatham et al. 2012). Elevated temperatures can also affect the development of pollen tubes. In Gossypium hirsutum L., pollen tubes stressed by high temperatures germinate earlier than controls but the rate of tube growth is lower; however, fertilization efficiency is not affected (Snider et al. 2011a). Negative effects on pollen tube growth may depend on the availability of sugars in the pistils (Snider et al. 2011b). In Nicotiana tabacum L., heat-stressed pollen tubes showed a temperature-dependent reduction in tube growth with changes in the accumulation of membranes, lower vesicle production and swelling of mitochondria (Kandasamy and Kristen 1989). Negative effects on pollen viability and germination have also been reported in strawberry (Ledesma and Sugiyama 2005) and in Pisum sativum L. (Petkova et al. 2009). Several tests performed on pollen development and growth suggest that pollen might be a suitable biomarker for assessing cultivars resistant to high temperature (Liu et al. 2006). The pollen tube is a tip-growing cell (Cole and Fowler 2006), in which the apical region contains a large amount of Golgi-derived secretory vesicles that will fuse with the plasma membrane providing new lipids, membrane proteins and cell wall proteins to the growing tube. The apical domain also contains a large number of molecules that polarize the pollen tube (Kost 2008). The apical polarization affects the arrangement of the cytoskeleton (Zhao and Ren 2006), which in turn regulates the trafficking of organelles and vesicles in the pollen tube (Zhang et al. 2010). The cytoskeleton is organized through the activity of several associated proteins (Staiger et al. 2010) that allow the arrangement of distinct cytoskeletal arrays. For example, the so-called actin fringe is a boundary between the subapical and apical region of pollen tubes that is likely to focus secretory vesicles at the fusion sites (Dong et al. 2012), a prerequisite for assembly of the pollen tube cell wall. Proper organization and dynamics of the cytoskeleton are required to produce functional pollen tubes. Despite this, little information is available on the response of cytoskeletal elements to heat stress, although the cytoskeleton has often been considered a target of heat stress (Kang et al. 2010). Root cells of Arabidopsis thaliana L. are capable of surviving a short-lived thermal stress showing a complete recovery of the cytoskeleton after initial depolymerization (Muller et al. 2007). Injuries to the cytoskeleton are usually observed after incubation at 40–42 ———————————C. Below this value, neither microtubules nor actin filaments are damaged (Smertenko et al. 1997). In BY-2 (Bright Yellow-2) tobacco cells, actin filaments are depolymerized by heat shock whereas mild heat stress has no effects (Malerba et al. 2010). Wang et al. (2012) reported the expression of heterodimeric proteins of Arabidopsis that bind to and ‘‘cap’’ the ends of actin filaments, likely functioning as pre-stress factors. These proteins are expressed in many plant tissues in response to thermal stress and might provide a molecular tool for development of thermo-tolerance. In eukaryotic cells, thermal denaturation of cytoskeleton proteins is likely either prevented or repaired by heat shock proteins (HSPs), a large family of molecular chaperones. Both microtubules and HSP90 from animal sources can interact with each other and HSP90 might refold denatured tubulins but it may not dissolve protein aggregates (Weis et al. 2010). Correspondingly, small HSPs can prevent aggregation of denatured actin subunits (Pivovarova et al. 2007). In favor of a HSP-based protective activity, experimental evidence indicates the interaction between HSPs and cytoskeletal proteins such as tau (Patterson et al. 2011) and kinesin (Parrotta et al. 2013). These findings suggest that HSPs might either increase the dynamics of the cytoskeleton or support the correct folding of new subunits (Silflow et al. 2011). We investigated the effects of heat stress on pollen tubes by heat-stressing pollen grains and monitoring the effects on pollen tube germination and cytoskeleton. Accordingly, we evaluated how heat stress applied to pollen grains may have consequences on the developing pollen tubes. This analysis might also suggest how recovery mechanisms carried out by pollen grains contribute to withstanding heat stress. The functional hypothesis is based on the importance of pollen tubes in plant reproduction and on the use of pollen tubes as an excellent cell model. In addition to biochemically and cytologically evaluating the effects of heat stress

on the cytoskeleton, we analyzed two cytoskeleton-based mechanisms: vesicle dynamics and distribution of sucrose synthase. Sucrose synthase is a metabolic enzyme but is also an actin-binding protein (Winter et al. 1998), and is involved in cell wall assembly by providing metabolites for the synthesis of cellulose and callose (Zheng et al. 2011). Moreover, sucrose synthase can also be a preferential target of heat stress (Pressman et al. 2006) because content and activity of the enzyme change in response to heat stress.

MATERIALS AND METHODS

Experimental protocol for heat-stressing pollen grains

After hydration at room temperature overnight in a humid chamber, tobacco pollen was placed within petri dishes and stressed by heat treatment at 35°/37°/40°C for three hours using incubation chambers set at predefined temperature. Control pollen was kept at room temperature during heat treatment. Both control and heat-stressed pollen was germinated in BK medium (Brewbaker and Kwack 1963) supplemented with 12% sucrose for three hours. All samples were subsequently subjected to investigations.

Extraction of proteins from cytosol, membrane and cell wall fractions

After germination, pollen tubes were collected by low-speed centrifugation and washed with HEM buffer (50 mM Hepes pH 7.5, 2 mM EGTA, 2 mM $MgCl_2$) containing 12% sucrose. Pollen tubes were lysed in a cold room using a Potter-Elvejhem homogenizer (40 strokes); the lysis buffer was HEM supplemented with protease inhibitors and 1 mM DTT. Samples were centrifuged at 500 g for 10 min (4°C). The supernatant was removed and centrifuged at high-speed (100000 g for 45 min at 4°C). The resulting pellet (e.g. the membrane fraction) was resuspended in either sample buffer for 1-D electrophoresis or RB buffer for 2-D electrophoresis; samples were then centrifuged at 15000 g for 20 min in a microfuge and the supernatant was directly used. The supernatant from the high-speed centrifugation (e.g. the cytosolic fraction) was precipitated in 4 volumes of 20% TCA in cold acetone for 2 hours at -20°C; precipitated proteins were washed in cold acetone and then resuspended in suitable buffers for either 1-D or 2-D electrophoresis.

The pellet from the initial low speed centrifugation (e.g. the cell wall protein fraction) was washed several times with HEM buffer to remove contaminating proteins. The last pellet was directly incubated with buffer for either 1-D or 2-D electrophoresis.

Subfractionation of cell wall proteins

Cell wall proteins were extracted using three different conditions in order to obtain proteins weakly bound to the cell wall (0.15 M NaCl), proteins bound to the wall by stronger ionic interactions (1 M NaCl) and proteins strongly bound to the cell wall (possibly by hydrophobic interactions, 2% SDS) (Borderies et al. 2003). After stressing and germination, pollen tubes were collected, washed and lysed. The lysate was centrifuged at 10000 g for 15 min at 4°C. The pellet was resuspended in 0.15 M NaCl in extraction buffer and incubated (each incubation was performed for 30 min with 400 RPM agitation in a thermomixer set at 25°C). Samples were centrifuged at 10000 g for 15 min at 25°C. The supernatant was recovered while the pellet was repeatedly washed with the same buffer to elute unspecifically binding proteins. Subsequently, pellets were resuspended with 1 M NaCl in extraction buffer and incubated as above; following centrifugation at 10000 g for 15 min, the supernatant was retrieved and the pellet was repeatedly washed with the same buffer and then with a no-salt buffer to decrease salt concentration. Samples were resuspended and incubated in 2% SDS in extraction buffer, centrifuged at 10000 g for 15 min to retrieve the final supernatant. All supernatants were precipitated in 20% TCA-acetone overnight at -20°C. The day after, samples were centrifuged at 16000 g for 15 min at 4°C and pellets were washed with cold acetone and centrifuged again at 16000 g for 15 min at 4°C. The final pellets were re-suspended in a small volume of denaturation buffer for 1-D electrophoresis.

Determination of protein concentration

The protein concentration of samples was determined using a commercial kit (2-D Quant Kit, GE HealthCare). The protocol was performed exactly as described in the instruction manual using BSA as reference. Each sample was analyzed in three replicates.

Electrophoresis, immunoblotting and image acquisition

Separation of proteins by 1-D electrophoresis was performed on pre-cast 10% Criterion XT gels (Bio-Rad) using a Criterion cell (Bio-Rad). Run was done with a Power Pac Bio-Rad 300 at 200 V for approximately 45 min. Gels were stained with Bio-Safe Coomassie (Bio-Rad).

Transfer of proteins from gels to nitrocellulose membrane was performed using a Trans-Blot Turbo Transfer System (Bio-Rad) according to the manufacturer's instructions. Quality of blotting was determined by checking the transfer of Precision pre-stained molecular standards (Bio-Rad). After blotting, membranes were blocked overnight at 4°C in 5% ECL Blocking Agent (GE HealthCare) in TBS (20 mM Tris pH 7.5, 150 mM NaCl) plus 0.1% Tween-20. After washing with TBS, membranes were incubated with the primary antibody for 1 h. For labeling tubulin, we used the mouse monoclonal anti-tubulin B-5-1-2 from Sigma, diluted 1:5000. For actin, we used the mouse monoclonal anti-actin 10B3 from Sigma diluted 1:3000. For immunodetection of sucrose synthase, we used a rabbit polyclonal against maize sucrose synthase (Heinlein and Starlinger 1989) diluted 1:1000. Subsequently, membranes were washed several times with TBS and then incubated for 1 h with peroxidase-conjugated secondary antibodies. Specifically, we used an anti-mouse IgG (Bio-Rad, diluted 1:5000), a goat anti-rabbit IgG (Bio-Rad) diluted 1:3000, and a goat anti-rat (Chemicon International) diluted 1:3000. After rinsing the membranes with TBS, the immunological reactions were visualized with Immun-Star (Bio-Rad). Images of gels and blots were acquired using a Fluor-S apparatus (Bio-Rad) and analyzed with the Quantity One software (Bio-Rad). Exposure times were 30-60 seconds for blots and 5-7 seconds for Coomassie-stained gels.

2-D electrophoresis and spot analysis

Two-dimensional electrophoresis of proteins was performed using 11-cm Immobiline Dry Strip (GE Healthcare) with a pH 4-7 linear gradient. Strips were rehydrated in the solubilization buffer (40 mM Tris, 8 M urea, 2 M thiourea, 2% CHAPS, traces of Bromophenol blue) to which we added 18 mM DTT and IPG buffer (20 µl/ml). Samples were dissolved at 2 mg/ml concentration in the solubilization buffer. Strips were rehydrated overnight in Immobiline Dry Strip Reswelling Tray (GE) and covered with the Dry Strip Cover PlusOne (GE HealthCare) to avoid dehydration of strips. A 4-step run was done using a cooled Multiphor II plate and an EPS 3500 XL power supply: from 0 V to 300 V in 20 minutes, 300 V for 1 h 30 min, a linear gradient from 300 V to 3500 V for 1 h 30 min, 3500 V for 3 h 30 min. Strips were stored at -80°C or used immediately. In both cases, strips were equilibrated for 15 minutes in equilibration buffer (50 mM Tris-HCl pH 8.8, 6 M urea, 30% glycerol, 2% SDS, Bromophenol blue, 10 mg/ml DTT). For the second dimension, we used precast Criterion XT 10% gels (Bio-Rad) on which strips were placed and held in the correct position by an agarose layer. Electrophoretic run was performed with a Criterion Cell (Bio-Rad) at 200 V. Gels were stained with Coomassie Bio-Safe (Bio-Rad) or alternatively transferred onto nitrocellulose membranes for immunoblotting.

Analysis of spots in 2-D gels and blots was performed using the Spot Detection Wizard of PDQuest (Bio-Rad) by initially selecting the weakest protein spot and the larger protein clusters. Subsequently, spot analysis was improved manually by adding unidentified spots and by removing incorrect signals. After creating a Master (virtual) gel, spots were matched to determine qualitative and quantitative differences. For immunoblotting, acquisition and measurements were made using the same conditions (exposure time,

selection of parameters and scan settings) to minimize the variability of results. Image acquisition was followed by background subtraction. Spot quantization was made using the Spot Volume command of the Quantity One software, which returned results in the form of Adjusted Volume. For statistical analysis of immunoblots, each experiment was repeated 2 times while measures were performed 3 times by different operators. To compare data, we used the Student t-tests of Microsoft Excel. Differences were significant for $P \leq 0.05$ and for $P \leq 0.01$ (as indicated by one or two asterisks in the graphs).

Kymograph analysis of pollen tubes

Pollen tubes were observed using an inverted microscope (Nikon) Diaphot TMD with a 40X objective. Video sequences were captured using a CCD camera C2400-75i Hamamatsu (Hamamatsu Photonics) connected to Argus-20 (Hamamatsu) and then to a video capture system (Cai et al. 2000). Pollen tubes were monitored for about three hours and video clips were captured in MPEG-2 at a resolution of 720×576 pixels using the software PCTV Center. MPEG-2 files were converted into AVI (MJPEG compression) by the software VirtualDub (http://virtualdub.org/) and then opened in ImageJ software (http://rsbweb.nih.gov/ij/index.html). Video sequences were analyzed by the plug-in Kymograph to measure the speed of moving objects in a series of images. We analyzed and measured the gray values in a given region of interest (ROI) selected manually for each frame in the image series. A new image (a kymograph or space-time graph) is generated, in which the X-axis is the time axis (the unit is represented by the frame interval) and the Y-axis indicates the movement rate of ROI (the unit of measurement is the distance traveled by the object in pixels). The speed of objects can be measured directly by the plug-in. At least 20 pollen tubes for each sample were analyzed.

Fluorescence microscopy and measurement

For actin labeling, pollen tubes of tobacco were grown for 3 hours, fixed and permeabilized in 100 mM Pipes pH 6.9, 5 mM $MgSO_4$, 0.5 mM $CaCl_2$, 0.05% Triton X-100, 1.5% formaldehyde, 0.05% glutaraldehyde for 30 min (Lovy-Wheeler et al. 2005). Samples were washed twice with the same buffer described above except that the pH was 7 and it contained 10 mM EGTA and 6.6 µM Alexa 543-phalloidin (InVitrogen). Samples were placed on slides and covered with a drop of Citifluor.

Indirect immunofluorescence microscopy in pollen tubes was performed according to standard procedures (Persia et al. 2008; Cai et al. 2011). Briefly, the protocol involves the following steps. After fixation with 3% paraformaldehyde in PM buffer (50 mM PIPES, pH 6.9, 1 mM EGTA, 0.5 mM $MgCl_2$) for 30 min, samples were washed with PM for 10 min and then incubated with 1.5% cellulysin for 7 min in the dark. After two washes with PM, samples were incubated with the primary antibodies. The anti-sucrose synthase antibody (Heinlein and Starlinger 1989) was used at 1:100 dilution while the anti-tubulin B-5-1-2 was used at 1:300. Antibodies were incubated at 4°C overnight. Following two washes with PM, samples were incubated with either goat anti-rabbit or goat anti-mouse secondary antibodies conjugated to Alexa Fluor 488 (Invitrogen) diluted 1:150 for 45 min in the dark. After two washes in PM, samples were placed on slides and covered with a drop of Citifluor. For actin and antibody labeling, observations were made using a microscope Zeiss Axio Imager with a 63x objective. Images were acquired with an AxioCam MRm camera using the software AxioVision. Images of higher quality were obtained using the Apotome module. In controls, primary antibodies were omitted.

To evaluate the orientation of actin filaments in the pollen tubes, we used the plugin FibrilTool under ImageJ (Boudaoud et al. 2014). The plugin allows the quantitative description of the anisotropy of fibers and their average orientation in cells. For pollen tubes, we selected three distinct areas: the hemispherical dome, the following 5 µm segment (approximately the subapex region) and two large segments in the pollen tube

shank. We applied the predefined settings of the plugin. Analysis was performed on at least 10 different randomly-selected pollen tubes (for both control and treated samples) with equivalent length.

The vesicular trafficking at the pollen tubes apex was monitored by analyzing the GFP-labeled Rab11b protein. Rab11b is a member of the Ras superfamily that probably regulates the traffic of Golgi vesicles to the cell membrane and the recycling of vesicle at the pollen tube apex (de Graaf et al. 2005). Tobacco plants stably transformed with Rab11b-GFP were kindly provided by Prof. Alice Cheung (Department of Biochemistry and Molecular Biology, University of Massachusetts, Amherst) and seeds were treated as described in Cai et al. (2011). Pollen tubes germinated from heat-stressed pollen grains were observed by fluorescence microscopy. The signal intensity was measured in 2 µm-segments starting from the pollen tube tip with ImageJ software.

Labeling of cell wall-secreted material was performed using the PI staining as described in Rounds et al. (2014). It is suggested that PI binds pectin and that it might indicate the deposition of new cell wall material, mainly pectins.

Immunogold electron microscopy and particle counting

Immuno-gold labeling on tobacco pollen tubes was performed according to the protocol described in Li et al. (1995). The antibody to sucrose synthase was used at the dilution of 1:200 in 50 mM Tris-HCl pH 7.6, 0.9% NaCl, 0.1% Tween-20, 0.2% BSA. The goat secondary antibody was conjugated with 15 nm-gold particles (BioCell). Images were captured with the transmission electron microscope (TEM) Philips Morgagni 268 D set at 80 kV and equipped with a MegaView II CCD Camera (Philips Electronics, Eindhoven, The Nederlands). Samples were incubated with a blocking serum for 20 min at room temperature to prevent binding to nonspecific sites. Sections were incubated with the primary antibody for 1 hour and then washed (3-4 times) in 50 mM Tris-HCl pH 7.6, 0.9% NaCl, 0.1% Tween 20 for 30 min. After drying, samples were incubated with the gold-conjugated secondary antibody for 15 min at room temperature. After washing for 30 min and in H_2O for 10 min, sections were counterstained with 2% uranyl acetate in H_2O for 10-20 min, carefully washed in H_2O for 15 min and then counterstained with lead citrate for 5-10 min. For counting gold particles, we saved several EM images and each image was imported into ImageJ. Scaling was done using the scale bar generated by the microscope software (AnaliSYS). Images were subjected to threshold to easily visualize gold particles. Using the free-hand selection tool, we selected the cell wall region and the counting of gold particles was automatically done by the software. Simultaneously, we also measured the area of the cell wall region.

RESULTS

Germination rate and length of pollen tubes are affected by heat stress

We initially measured the germination rate and length of pollen tubes (Figure 1) to provide information on the effects exerted by heat stress on two basic features of pollen tubes. Changes to the germination rate and length of pollen tubes from heat-stressed pollen grains were discernable at the optical microscope when compared to controls. While untreated pollen tubes exhibited a typical germination rate and tube length (Figure 1A, top left), pollen grains stressed at three different temperatures (35°C, 37°C and 40°C) showed a comparable reduction in both germination rate and length. To statistically evaluate both parameters, we measured the germination rate and length of several pollen tubes (at least 50 for each condition) (Figure 1B-C) in the three experimental conditions. The germination rate decreased proportionally to the increasing of temperature. The most dramatic effect was at 40°C with the germination rate that did not exceed 20%. Comparable results were observed for tube length, which was significantly reduced at 35°C and at about one-third at 40°C (Figure 1C).

To separate the impact of heat stress on germination and tube extension rate, we performed a heat stress assay at 40 °C according to the protocol described above but we analyzed the germination rate and pollen tube length at different times (up to 4 h) (Fig. 2a, b). We found that the germination rate is significantly affected soon after the first hour of germination and that the negative impact of heat stress increased afterwards up to 4 h of analysis (Fig. 2a). Conversely, we found that the pollen tube elongation rate was less affected (Fig. 2b). This result is in accordance with the movement of generative cells, which was assayed to determine if generative cells were translocated and moved in pollen tubes after heat-stressing pollen grains. We measured the distance traveled by generative cells and we normalized the data to the pollen tube length. Results showed that the movement of generative cells was not affected by heat treatment of pollen grains (Fig. 2c, d, e). The percentage of germinating pollen tubes is considerably low after heat stress and this consequently affects the number of generative cells entering pollen tubes; however, when pollen tubes germinated for at least 4 h, generative cells moved into pollen tubes and covered a similar distance in comparison to control pollen tube.

The growth rate of pollen tubes was also analyzed by kymograph analysis. In control pollen tubes (Figure 3A), the growth speed was constant as shown by the linearity of kymograph profile. The typical oscillation of growth (slower phases of growth preceded/followed by peaks of fast growth) can be seen in the inset. When pollen grains were heat-stressed before germination (Figure 3B), the growth speed is still constant as shown by kymograph linearity but significantly lower than controls. In addition, we did not detect any indication of oscillated growth.

The relative quantity of actin, tubulin and HSP70 is slightly affected by heat stress

Members of the heat-shock protein family are common players in the response of eukaryotic cells to heat stress. Therefore, we analyzed the presence and abundance of one subfamily, the HSP70 specifically. Immunoblot analysis with HSP70 antibody on both cytosolic and membrane protein fractions from control (RT, room temperature), 35°C and 40°C heat-stressed pollen extracts (Figure 4A) revealed comparable signals in both extracts. In all samples, the antibody cross-reacted with a single band around 70-75 kD. The signal intensity was generally higher in cytosolic fractions (lane 8, 9 and 10 in Figure 4B) than in membrane fractions (lane 11, 12 and 13). No quantitative differences between samples were observed because the measurement of blot intensity showed that the relative amount of HSP70 was comparable in the cytosolic protein fractions (S) with the exception of the 40°C treatment where the amount of HSP70 slightly decreased (Figure 4D). In membrane fractions obtained after heat treatment (P), the relative amount of HSP70 was unaffected (Figure 4D). We also checked the relative amount of tubulin and actin, the two main cytoskeletal proteins (Figure 4C). Immunoblot against tubulin and actin was performed on cytosolic proteins extracted from pollen tubes after heat-stressing pollen grains at 40°C. Tubulin was consistently found in both control (lane 1) and heat-stressed (lane 2) pollen although the amount in heat-stressed samples was seemingly lower. On the contrary, the amount of actin as detected by immunoblot with anti-actin antibody was very similar between control (lane 3) and 40°C-stressed cytosolic proteins (lane 4). Blot images were confirmed by relative quantization of signals (Figure 4E). The blot intensity of tubulin in 40°C-stressed samples (gray bar) was statistically lower than the amount of tubulin in untreated samples (black bar). Conversely, the amount of actin was invariable between heat-stressed and control samples (Figure 4E).

Heat-stressed pollen tubes accumulate different actin and tubulin isoforms

To deepen the results obtained after 1-D electrophoresis, we separated cytosolic proteins by 2-D electrophoresis (Figure 5A). Representative 2-D gels of cytosolic proteins from control (left) and 40°C-stressed pollen (right) along with a 4-7 pH gradient revealed a comparable spot pattern. However, several differences could be detected. The total number of spots in control and treated samples was equivalent but

about 10% of spots were found only in controls (examples indicated by arrows) and around 20% were typical of treated samples (as indicated by arrowheads). When examining common spots with significant differences (namely, spots showing an integrated density more than twice or less than half of corresponding spots in the other sample), we found that 15% of spots were over-expressed in heat-stressed pollen (examples indicated by circle). Correspondingly, about 18% of common spots were over-expressed in control pollen (examples indicated by box).

The analysis of tubulin by 2-D electrophoresis and immunoblotting revealed a certain number of differences (Figure 5B). When compared to controls (top panel), heat-stressed samples (bottom panel) showed a peculiar pattern of spots. While we detected three spots in control samples (pH range 4.5-5), spot 1 and 2 almost disappeared in heat-stressed samples and spot 3 increased considerably. In addition, four other spots were detected (spot 4, 5, 6 and 7). The relative quantification of single spots from three independent blots confirmed the analysis and highlighted the presence of new tubulin spots after heat stress (Figure 5C).

Immunoblot analysis with anti-actin antibody in both control (Figure 6A, top panel) and heat-stressed samples (bottom panel) showed that the isoform pattern of actin also changed. In control samples, we detected seven distinct spots ranging around pH 5.5-6. Spots were characterized by relative different intensities. In heat-stressed samples (bottom panel), we usually found the same protein spots already identified in controls with the addition of extra spots thereby reaching a total of 13 actin spots. Additional spots were found in both basic and acidic regions. When we relatively quantified the blot intensity (Figure 6B), spot 1 was essentially typical of controls whereas spots 8-13 were basically expressed in heat-stressed pollen. Other spots (from 2 to 7) might be considered as equivalent between the two test conditions (variations occurred within experimental error). Some spots (such as spot 1 in controls) appeared to split in two distinct spots (1 and 10 in stressed samples); other spots (such as 12 and 13) appeared as typical of stressed conditions.

Microtubules change drastically in response to heat stress while only the subapical actin array changes

Analysis of tubulin distribution revealed considerable changes to microtubule organization. In controls, the microtubule pattern was essentially comparable to the one described in the literature with microtubules lining along the main axis of pollen tubes, sometimes with helical arrangements (Figure 7A1-A2). In the apex, microtubules were usually absent and could be detected only up to 20-30 µm from the tip. The apical dome generally showed a diffuse signal likely indicating unpolymerized tubulin (Figure 7A3). In pollen tubes germinated from heat-stressed pollen grains, microtubules showed dramatic alterations because they appeared depolymerized and fragmented and even absent in some cases (Figure 7B1-B2). A diffuse signal was often detected. In the apex, we observed short, fragmented or dotted-like microtubules essentially distributed in the cell cortex (Figure 7B3).

We visualized actin filaments in control and pollen tubes from heat-stressed pollen grains to correlate the electrophoretic profile with the organization of this cytoskeletal component. Apparently, we did not observe clear differences between control and heat-stressed pollens. Actin filaments were arranged as short and irregular in the apical region while they were organized as longer longitudinal filaments in the pollen tube shank. To appreciate more subtle differences, we performed a software-based analysis of actin filaments using the plugin FibrilTool running under ImageJ (Figure 8A1-A4 for control; Figure 8B1-B4 for heat-stressed samples). The plugin can determine the anisotropy of filamentous structures such as actin filaments, microtubules and cellulose microfibrils. We subdivided pollen tubes into four district segments: the hemispherical dome (n. 1), the subsequent 5-µm segment (roughly corresponding to the subapex, n. 2) and two longer segments in the pollen tube shank (n. 3-4). Statistical analysis in the four segments show no clear differences in the anisotropy of actin filaments (Figure 8C) with the exception of the subapical domain

(segment 2). Here, the anisotropy of actin filaments was significantly higher in heat-stressed samples compared to controls. Conversely, other regions showed comparable values suggesting that the main difference in actin organization might occur in the subapex of heat-stressed pollen tubes.

Apex-localized vesicles are distributed differently

A differential organization of actin in the subapical region of pollen tubes might have consequences on the redistribution of membrane-bound structures, primarily secretory vesicles. To assess this, we used pollen tubes expressing a GFP-tagged Rab11b protein, which is associated with Golgi-derived vesicles. In controls, GFP-labelled vesicles accumulated consistently in the hemispherical dome with an inverted cone shape (Figure 9A). Superficially, the distribution of vesicles in heat-treated samples was comparable and no macroscopic differences were observed (Figure 9B). However, we also measured the fluorescence intensity of GFP-labelled vesicles in several 2-µm segments starting from the tip (Figure 9C). We observed statistically-significant differences from segment 5-6 to 10, corresponding to about 10 to 20 µm from the tube tip. In this area, the fluorescence intensity was significantly lower than controls suggesting that a smaller amount of Golgi-derived vesicles accumulate in the subapex/shank of pollen tubes.

As an additional indicator of vesicle-based secretion, we also monitored the PI labelling of pectins. In controls, PI-stained pectins mostly accumulate in the apical and subapical cell wall. This pattern is consistent with the typical distribution of newly-synthetized and secreted pectins (Figure 9D with inset). Unlike controls, pollen tubes from heat-stressed pollen grains showed a remarkable difference as PI-labelled pectins do not accumulate with a gradient-like distribution. The content of PI-labelled pectins was relatively similar between the apex/subapex and the shank of pollen tubes indicating no preferential secretion/accumulation of newly-synthetized pectins (Figure 9E1-E2). Measurement of PI-labelled pectins along the cell border of different pollen tubes showed that in controls PI-labelled pectins accumulate primarily in the apex/subapex (roughly corresponding to the first 20 µm of pollen tubes) (Figure 9F). In heat-stressed samples, this gradient-like distribution is lost and pectins accumulate in different regions.

The marker protein sucrose synthase accumulates differently in cell compartments

As the cytoskeleton is the track system along which vesicles and organelles move, we analyzed one exemplifying protein (sucrose synthase) whose presence, relative abundance and distribution is dependent on the activity of both cytoskeleton and membrane system. The rationale is that the vesicle-based delivery of proteins might be affected by heat-induced alterations to the cytoskeleton.

At first, we investigated the distribution of sucrose synthase in control and heat-stressed pollen tubes by immunocytochemical analysis (Figure 10). Controls (A) showed the typical cortical distribution of the enzyme, less intense in the apical region and gradually more intense in distal regions; as described in the literature, sucrose synthase of pollen tubes is localized essentially in the cell edge presumably in association with the plasma membrane and cell wall. The distribution of sucrose synthase in heat-stressed samples was remarkably different because the enzyme was also consistently found in the cytosol as a diffused and irregular signal. Signal aggregates were often observed (arrows) (Figure 10B, C, D). The level of cortex-associated enzyme was usually lower in comparison to controls. Apparently, the heat shock can induce a substantial redistribution of sucrose synthase, which seems to lose its typical cortical localization and appears to aggregate inside the cell.

To get more information on the changes of sucrose synthase distribution, we also analyzed the relative content of the enzyme by immunoblot analysis on proteins extracted from the cytosolic, membrane and cell wall compartments (Figure 10E). Blot results confirmed that sucrose synthase in heat-stressed samples accumulated more consistently in the membrane fraction and in the cytosol but much less in the

cell wall fraction. This suggests that the heat shock of pollen grains caused a redistribution of sucrose synthase in pollen tubes.

We focalized our attention on the cell wall-associated protein fraction, which were isolated by a sequential extraction protocol (Figure 11A) based on the serial washing with 0.15 M NaCl, 1 M NaCl and 2% SDS. We compared the control incubated at room temperature (RT) to the 40°C-stressed sample (HS). Samples were similar in polypeptide composition (differences are indicated by dots for lanes 1, 2 and 6) but specific changes were more evident when proteins were assayed by immunoblot (Figure 11B). Antibodies to sucrose synthase (Sus) revealed that the cell wall-associated protein decreased substantially in heat-stressed samples extracted by 0.15 M NaCl and 1 M NaCl. A statistically significant reduction in NaCl-extracted protein fractions was confirmed by measurement of blot intensity for sucrose synthase (Figure 11C). The signal of sucrose synthase in the 2% SDS fraction is neglectable in both cases.

Differential accumulation of sucrose synthase corresponds to an altered distribution

To get more information on the localization of sucrose synthase in relation to heat treatment, we analyzed the subcellular distribution of the enzyme by immunogold labeling techniques (Figure 12). In control pollen tubes, sucrose synthase was found essentially in association with the plasma membrane (black arrow) and with the cell wall (white arrow). The two images (Figure 12A-B) were taken in the subapical region of pollen tubes. When samples were heat-stressed at 40°C (Figure 12C-E), gold particles were mostly found in association with intracellular membranes. We observed gold particles in association with the endoplasmic reticulum (C, arrow) but most of gold particles were found on the edge or just within vesicular structures (D, arrow). We do not know the identity of such membrane-bound structures but we hypothesize they may represent components of the endosomal/vacuolar system. One of the most striking difference with controls was represented by the very low number of gold particles in association with the plasma membrane or in the cell wall of pollen tubes (E, subapical region). Gold particles are conversely detected in the cytoplasm.

To get more deeply into differences, we measured the number of gold particle into the cell wall of both control and treated samples. We found a consistent difference because controls exhibited 78 ± 12 gold particle per μm^2 while stressed samples showed only 29 ± 8 gold particle per μm^2. The heat-stressed samples reasonably contained a lower level of sucrose synthase in the cell wall.

DISCUSSION

Heat stress can affect a number of cellular and physiological processes ranging from cell growth to macromolecule interactions. As the increase in global temperature is ongoing, understanding how heat stress can affect cell mechanisms is important for selecting plants more suitable for a changing environment.

Reproduction is a critical step in the life cycle of every living organism including plants and it is known that heat stress can affect pollen development and therefore can reduce plant fertility (Lu et al. 2009; Zinn et al. 2010). Although it is not clear in detail how heat stress affects pollen tube development, fertilization is dramatically reduced by heat stressing pollen germination and pollen tube growth (Zinn et al. 2010). The literature reports that heat stress can affect two important processes in the formation of pollen grains, microsporogenesis and microgametogenesis, and also cause histological and cytological defects in anther tissues (Hedhly 2011). The severity of male infertility depends on the developmental stage affected by thermal stress, with the most sensitive stages being meiosis and the last phase of mitosis (Saini et al. 1983; Vara Prasad et al. 2001; Vara Prasad et al. 2003). Injuries can lead to reduced seed production (Young et al. 2004) and fruit-set. At the level of pollen tubes, preliminary analysis on tobacco showed that high temperatures decreased tube growth by about 50% at 35°C and almost completely at 40°C or above. Heat treatment induced several ultrastructural changes on the organization of endomembranes such as the rough endoplasmic reticulum, vesicles and Golgi bodies, and mitochondria (Kandasamy and Kristen 1989). Effects

on pollen tubes at the level of germination rate and tube length might also depend on the species as well as on the cultivar analyzed (Ledesma and Sugiyama 2005). Several studies carried out on pollen tubes suggested that the male gametophyte can be used for selecting plant species more tolerant to heat stress (Liu et al. 2006; Petkova et al. 2009).

In the present study, we analyzed the development of pollen tubes when heat stress is applied to pollen grains. Information indicate how pollen tubes might suffer from treatment of pollen grains and how pollen grains might repair damages in order to produce functional pollen tubes. We specifically focused on the cytoskeleton and protein delivery. The cytoskeleton is critical for many cellular processes. In pollen tubes, it supports growth by modulating the delivery of several components to the apical domain and by regulating the proper assembly of the cell wall (Cai et al. 2014). We consequently monitored how heat stress affects the expression and arrangement of cytoskeletal proteins and the delivery of proteins targeted to specific cell sites. We found that heat stress affected both pollen tube germination and growth and that actin filaments and microtubules are affected in terms of isoform accumulation and organization. These changes likely reflect on the dynamics of organelle movement, which therefore might have consequences on the delivery of proteins.

In this work, analysis of HSP70 was essentially performed as control. Several data report that HSPs are not involved in the response of pollen grains to heat stress. For example, it was shown that the expression of HSP100 is not thermoinducibile in mature pollen (Young et al. 2001). This is consistent with the evidence that other HSPs (such as HSP90, HSP70 and HSP60) are only expressed during early stages of pollen development (Marrs et al. 1993; Magnard et al. 1996). Consequently, the expression of HSP100 and of other HSPs in mature pollen is likely insufficient to counteract the effects caused by heat stress (Mascarenhas and Crone 1996). Here, the content of HSP70 does not change during heat treatment in both cytosolic and membrane compartments of pollen tubes. This finding suggests that HSPs are not critically involved in protecting the pollen tube proteome from heat stress. Another interpretation is that additional mechanisms activated at the level of pollen grains might be sufficient to allow a certain rate of tube germination; consequently, higher levels of HSP70 are no more requested in pollen tubes.

The current literature reports several data on the susceptibility of actin filaments to heat stress. It should be considered that most of data were obtained by observing actin filaments under direct stress conditions whereas in the present study we analyzed actin dynamics after heat stress. In *Arabidopsis thaliana*, thermal stress can induce drastic rearrangement of the actin cytoskeleton, which can recover its original conformation upon cessation of heat treatment. This suggests that damages induced by heat shock are not permanent and that actin filaments are sufficiently dynamics to return to the initial organization (Müller et al. 2007b). Comparable effects were also described in tobacco BY-2 cells in which heat shock affected the polymerization state of actin filaments and also induced a reduction of actin content after 16 hours of treatment (Malerba et al. 2010b). In our study, we did not observed reduction of actin content but rather a change in the utilization of actin isoforms. Changing the actin isoforms might be an adaptation of cells to heat stress that occurs before pollen tubes germinate. Up- and down-regulation of actin isoforms have been reported in non-plant systems such as marine invertebrates of the Ciona genre under heat shock treatment (Serafini et al. 2011). This suggests that utilization of more adaptive actin isoforms might be a strategy used to counterbalance the effects induced by heat treatment. Accumulation of specific actin isoforms might not be specific for heat stress because it was also observed in soybean seedlings subjected to drought-stressed (Mohammadi et al. 2012).

Pollen tubes that germinate from heat-stressed pollen grains exhibited a comparable content of actin and a similar actin organization. However, small but critical differences might be detected in the subapical region of pollen tubes. Here, actin filaments exhibited a higher anisotropy resulting in more directed actin filaments. Although this might be a minor difference, the organization of actin filaments in the subapex is critical because this area is the boundary between the long actin filaments in the shanks and the more

dynamic actin network in the apex (Cardenas et al. 2005). Actin filaments in the subapex are likely involved in controlling the spatial distribution of organelles and in focusing secretory vesicles in the apical dome. In most species, the subapex contains the actin fringe (in tobacco the actin fringe is closer to the tip), a dynamic ordered actin structure that oscillates in relationships with pollen tube growth. The dynamics of actin fringe likely controls the speed of pollen tube growth (Lovy-Wheeler et al. 2005; Dong et al. 2012). The higher level of anisotropy as observed in our study indicates that the actin fringe might be less dynamic. This could impair the way the pollen tube grows and this hypothesis is confirmed by the absence of growth oscillation as observed using kymograph analysis. The absence of the fast growth step might reduce the overall extension rate of pollen tubes thereby causing a strong reduction in tube growth.

It is currently difficult to correlate the changes in actin isoforms to the different anisotropy of actin filaments in the subapex. No data are available on the utilization of different actin isoforms in the pollen tube. Therefore, we may simply speculate that changes in actin isoforms may somewhat impair the proper organization of actin in the subapex. An orchestra of several actin-binding proteins, which might bind differently to specific actin isoforms, performs regulation of actin dynamics in the apex/subapex of pollen tubes.

This small but critical difference in actin organization unlikely have important consequences on organelle movement. The distribution of actin filaments in the shanks is not affected and some preliminary observations indicate that the pattern and speed of organelles is not modified (data not shown). Conversely, distribution of vesicles in the apex might suffer from changes to the subapical actin organization. In support of this, Rab11b-labelled vesicles showed a moderate change of distribution as they are more/less focused in the subapex. Although not extremely evident, difference in vesicle distribution might reflect changes to the dynamics of vesicles in the apex thereby contributing to reduce the tube growth rate. In support of this hypothesis, the actin fringe has been proposed as a regulator of organelle dynamics at the apex/subapex interface (Hepler and Winship 2014). One hypothesis suggests that vesicles might accumulate consistently in the tube apical side corresponding to a less extended actin fringe. Therefore, if the dynamics of actin fringe is altered, vesicle focusing and fusion might also be impaired.

An indirect confirmation of altered vesicle distribution and dynamics can be found in changes to pectin distribution. Although PI is not a specific marker of pectins, its capacity to co-localize with newly-synthetized cell wall in pollen tubes makes PI an excellent tool to visualize the deposition of pectins (that are the first cell wall component to be secreted) (Rounds et al. 2014). Heat-stressing pollen grains resulted in an altered profile of pectins in the apex of pollen tubes. While pectins accumulate mostly in the cortical apex and subapex of control pollen tubes, heat stress induced a uniform distribution of pectins. Although the correlation with altered vesicle dynamics is not immediate, the change in pectin deposition matches the absence of pulsed (oscillated) growth of pollen tubes. An irregular deposition of pectins is often correlated with changes to tube growth because a correct pulsed growth is directly dependent on the interchange between vesicle-based secretion of methyl-esterified pectins and conversion into acidic pectins (McKenna et al. 2009; Fayant et al. 2010; Biagini et al. 2014). Consequently, pollen tubes from heat-stressed pollen grains show non-pulsed growth that might be related to changes of the subapical actin array.

It is not known how microtubules are involved in tube growth. Nevertheless, depolymerization of microtubules might affect the oscillation rate of pulsed growth (Geitmann et al. 1996). Consequently, we analyzed the pattern of tubulin isoforms by 2-D electrophoresis and the distribution of microtubules. Results observed in control and heat-stressed samples were in line with changes detected for actin isoforms. Heat stress at the level of pollen grains might induce a different utilization of tubulin isoforms in pollen tubes, which may highlight an adaptation of cells to different thermal conditions. In tobacco suspension cells, treatment at 42°C caused severe damages to different microtubule arrays. Damages are reversible and are not correlated to the activity of heat- shock proteins (Smertenko et al. 1997). Therefore, microtubules appear susceptible to heat stress. Recovery of microtubules in a time-dependent manner was also observed in

epidermal root cells of Arabidopsis thaliana suggesting that the alteration of microtubules is not an irreversible effect and that tubulin subunits are not permanently modified (Müller et al. 2007a). Nevertheless, a protective activity of HSPs might be required to facilitate the assembly of microtubules. In animal systems, HSP90 was shown to protect tubulin subunit from denaturation thus facilitating the correct aggregation of subunits into nascent microtubules (Weis et al. 2010). Comparable studies in the alga Chlamydomonas indicated that the a HSP70/HSP40 chaperone might be required for the thermal stability of microtubules (Silflow et al. 2011). Evidences that different tubulin isoforms might be essential for the survival of heat-stressed cells are lacking; however, different expression patterns of tubulin were recorded when root cells of rice are subjected to drought stress (Mirzaei et al. 2012). This example indicates that altered growth conditions might affect the expression of tubulin leading to the utilization of isoforms most adapted to stress conditions. Unlike heat stress, more information are available for cold stress. In that case, cold treatment resulted in depolymerization of microtubules and formation of more resistant cold-stable microtubules; this implies changes in the expression pattern of tubulin (Abdrakhamanova et al. 2003). A different tubulin pattern in 2-D electrophoresis might result from either a different gene expression or post-translational modification of pre-expressed tubulins. In plants, different tubulin genes are expressed according to specific developmental pathways while post-translational modifications are often used for cell-based functions such as interactions with microtubule-associated proteins (Parrotta et al. 2013a). Post-translational modifications include addition/removal of different chemical groups such as phosphate or tyrosine. Modification of pre-existing tubulins might affect the way microtubules interact with other proteins and, more generally, the behavior and dynamics of microtubules. It is therefore expected that stressed cells might use different assortments of tubulins according to the different cell environment.

Changes to the cytoskeleton in terms of actin/tubulin isoforms and organization might have consequences on proteins whose localization depends on the cytoskeleton integrity and dynamics. Proteins might acquire a specific cell localization either because they are transported and delivered by cytoskeleton-interacting membranes or because they interact directly with the cytoskeleton. To assess such effect we analyzed a protein (the enzyme sucrose synthase) that is known to associate with cytoskeleton-interacting vesicles and with actin filaments (Cai et al. 2011).

Sugars and their metabolizing enzymes (like sucrose synthase) are critically involved in the response of plants to heat stress because sugar-metabolizing enzymes can change the level of sugars functioning as either protectant or signaling molecules (Ruan et al. 2010). Sucrose can act as osmoprotectant in maintaining the integrity of cell membranes under heat stress. In addition, the content of sucrose is directly correlated with the accumulation of starch in the pollen grain. In cereals, accumulation of starch is the result of complex enzymatic processes dependent on sucrose synthase and soluble starch synthase (Morell et al. 2001). High temperatures seem to reduce the activity of these enzymes (Sakurai et al. 2007). In general, thermal stresses causes down-regulation of several genes important for the development of the male gametophyte including invertase-encoding genes (Sato et al. 2006). Inhibition of invertase results in the accumulation of sucrose but in the lower availability of glucose and fructose, which might be conversely required for the synthesis of other carbohydrates necessary for the growth of pollen tubes.

Sucrose is cleaved in plant cells by two distinct enzymes, invertase and sucrose synthase. We investigated the content and distribution of sucrose synthase because the enzyme is associated with the vesicular compartment of pollen tubes (Persia et al. 2008; Cai et al. 2011), is involved in providing metabolites for the synthesis of cell wall polymers (Salnikov et al. 2003) and associates with the cytoskeleton (Winter et al. 1998). In addition, accumulation and activity of sucrose synthase may correlate with the heat stress response (Pressman et al. 2006). We found that sucrose synthase was affected in terms of content and distribution. A notable finding was the consistent decrease of sucrose synthase in the cell wall as confirmed by both immunoblot assays and microscopy analysis. This finding clearly shows that, after heat shock of pollen grains, sucrose synthase redistributes differently in pollen tubes.

Although sucrose synthase might take part in the response of plants to heat stress, the molecular details are not clear. In maize kernels, heat stress caused a reduction in the expression of sucrose synthase genes without affecting enzyme activity (Duke and Doehlert 1996). A non-significant change in sucrose synthase activity after heat shock was also reported for potato shoots (Lorenzen and Lafta 1996). No specific increase of sucrose synthase activity was detected after heat stressing the reproductive organs of thermo-tolerant lines of tomato (Li et al. 2011). In contrast, increase of sucrose synthase activity was reported during the development of tomato anther subjected to heat stress (Pressman et al. 2006). Accumulation of sucrose synthase was found in a thermo-tolerant *Agrostis* grass species suggesting that the hydrolyzing capacity of sucrose synthase may provide metabolites used as thermo- protectant factors (Xu and Huang 2008). Changes in sucrose synthase activity was also correlated with altered levels of starch in developing grains of wheat between heat-tolerant and heat-susceptible cultivars (Yan et al. 2008). In a comparable study in wheat, the activity of sucrose synthase fluctuated in accordance with the timing of heat stress by increasing at the beginning of heat treatment and decreasing in later stages of heat shock (Zhao et al. 2008). Another study in wheat pointed out that the activity of sucrose synthase could be repressed by treatment at high temperature (Asthir et al. 2013). A moderate increase of expression and activity of sucrose synthase was also described in alfalfa leaves subjected to heat stress (Mo et al. 2011). In the cambial zone of Populus tremula, heat stress also caused a decrease in sucrose synthase content (Durand et al. 2012) and decrease of sucrose synthase activity was described in chickpea (Kaushal et al. 2013). The enigmatic response of sucrose synthase is confirmed by analysis of tomato leaves subjected to heat stress; in such case, activity of sucrose synthase and sucrose phosphate synthase increased continuously but the activity of invertase decreased. Consequently, the content of fructose, glucose, and sucrose decreased but the content of starch increased in stressed plants (Zhang et al. 2012). Apparently, it is not yet possible to formulate a hypothesis applicable for all tissues/organs of plants.

In the pollen tube, starch is hydrolyzed to simple carbohydrates for supporting pollen tube growth. Therefore, the role of sucrose synthase is likely related to the catabolism of sucrose into UDP-glucose, which is required for the synthesis of both cellulose and callose. One hypothesis suggests that the biosynthesis of cell wall polymers might require a form of sucrose synthase associated with the plasma membrane and/or the cell wall (Persia et al. 2008; Brill et al. 2011). Consequently, synthesis of cell wall in tip-growing cells could determine the association of sucrose synthase with the plasma membrane or the cell wall. Under condition of heat stress, more energy could be required for the metabolism of pollen tubes and consequently less energy might be allocated to cell wall synthesis and growth. In Gossypium hirsutum pistils, pollen tube growth under heat stress is likely dependent on the availability of carbohydrates (Snider et al. 2011b) suggesting that the content of soluble carbohydrates inside the pollen tube is a critical parameter controlling tube growth. In the attempt to rebalance the carbohydrate content, sucrose synthase could be redirected to the cytoplasmic form or alternatively remained quiescent in the endomembrane system. By preventing the association of sucrose synthase with the plasma membrane or its secretion into the cell wall, pollen tubes might reduce the level of cell wall synthesis. It is known that the transition from membrane-associated to cytosolic sucrose synthase is dependent on the phosphorylation of specific amino acids (Hardin et al. 2004). Several evidences also suggest that the response of plants to heat shock is also articulated through changes in kinase/phosphatase activity targeted to HSFs (Mittler et al. 2012). Although we did not measure the level of phosphorylated proteins, we may assume that the altered activity of kinases/phosphatases might affect the distribution of sucrose synthase. In addition, phosphorylation also regulates the binding of sucrose synthase to actin filaments, which may in turn affect the intracellular localization of the enzyme (Duncan and Huber 2007). Changes to vesicle delivery might also affect the distribution of sucrose synthase and therefore might impair the synthesis of cell wall. This suggests that changes in the distribution of sucrose synthase may reflect an adaptation of pollen tubes to new environmental conditions imposed by deactivation/inhibition of metabolic pathways at the level of heat-stressed pollen grains.

References

Abdrakhamanova A., Wang Q.Y., Khokhlova L., & Nick P. (2003) Is Microtubule Disassembly a Trigger for Cold Acclimation? Plant and Cell Physiology 44, 676-686.

Allison I., Bindoff N.L., Bindschadler R.A., Cox P.M., De Noblet N., England M.H., Francis J.E., Gruber N., Haywood A.M., & Karoly D.J. (2009) The copenhagen diagnosis. The University of New South Wales Climate Change Research Centre, Sidney, Australia 60,

Asthir B., Bala S., & Bains N. (2013) Metabolic profiling of grain carbon and nitrogen in wheat as influenced by high temperature. 41, 230-242.

Biagini G., Faleri C., Cresti M., & Cai G. (2014) Sucrose concentration in the growth medium affects the cell wall composition of tobacco pollen tubes. Plant Reprod 1-16.

Borderies G., Jamet E., Lafitte C., Rossignol M., Jauneau A., Boudart G., Monsarrat B., Esquerre-Tugaye M.T., Boudet A., & Pont-Lezica R. (2003) Proteomics of loosely bound cell wall proteins of Arabidopsis thaliana cell suspension cultures: a critical analysis. Electrophoresis 24, 3421-3432.

Boudaoud A., Burian A., Borowska-Wykret D., Uyttewaal M., Wrzalik R., Kwiatkowska D., & Hamant O. (2014) FibrilTool, an ImageJ plug-in to quantify fibrillar structures in raw microscopy images. Nat Protoc. 9, 457-463.

Brewbaker J.L. & Kwack B.H. (1963) The essential role of calcium ion in pollen germination and pollen tube growth. Amer.J.Bot. 50, 859-865.

Brill E., van Thournout M., White R.G., Llewellyn D., Campbell P.M., Engelen S., Ruan Y.L., Arioli T., & Furbank R.T. (2011) A novel isoform of sucrose synthase is targeted to the cell wall during secondary cell wall synthesis in cotton fiber. PLANT PHYSIOLOGY 157, 40-54.

Cai G., Faleri C., Del Casino C., Emons A.M.C., & Cresti M. (2011) Distribution of callose synthase, cellulose synthase and sucrose synthase in tobacco pollen tube is controlled in dissimilar ways by actin filaments and microtubules. Plant Physiol 155, 1169-1190.

Cai G., Parrotta L., & Cresti M. (2014) Organelle trafficking, the cytoskeleton, and pollen tube growth. Journal of Integrative Plant Biology n/a-n/a.

Cardenas L., Lovy-Wheeler A., Wilsen K.L., & Hepler P.K. (2005) Actin polymerization promotes the reversal of streaming in the apex of pollen tubes. Cell Motil.Cytoskeleton 61, 112-127.

Cole R.A. & Fowler J.E. (2006) Polarized growth: maintaining focus on the tip. Curr.Opin.Plant Biol. 9, 579-588.

de Graaf B.H.J., Cheung A.Y., Andreyeva T., Levasseur K., Kieliszewski M., & Wu H.m. (2005) Rab11 GTPase-regulated membrane trafficking is crucial for tip-focused pollen tube growth in tobacco. The Plant Cell 17, 2564-2579.

Devasirvatham V., Gaur P.M., Mallikarjuna N., Raju T.N., Trethowan R.M., & Tan D.K.Y. (2013) Reproductive biology of chickpea response to heat stress in the field is associated with the performance in controlled environments. 142, 9-19.

Devasirvatham V., Gaur P.M., Mallikarjuna N., Tokachichu R.N., Trethowan R.M., & Tan D.K.Y. (2012) Effect of high temperature on the reproductive development of chickpea genotypes under controlled environments. 39, 1009-1018.

Dong H., Pei W., & Haiyun R. (2012) Actin fringe is correlated with tip growth velocity of pollen tubes. Molecular Plant 5, 1160-1162.

Duke E.R. & Doehlert D.C. (1996) Effects of heat stress on enzyme activities and transcript levels in developing maize kernels grown in culture. Environmental and Experimental Botany 36, 199-208.

Duncan K.A. & Huber S.C. (2007) Sucrose synthase oligomerization and F-actin association are regulated by sucrose concentration and phosphorylation. Plant Cell Physiol 48, 1612-1623.

Durand T.C., Sergeant K., Carpin S., Label P., Morabito D., Hausman J.F., & Renaut J. (2012) Screening for changes in leaf and cambial proteome of Populus tremula+ùP. alba under different heat constraints. 169, 1698-1718.

Fayant P., Girlanda O., Chebli Y., Aubin C.E., Villemure I., & Geitmann A. (2010) Finite Element Model of Polar Growth in Pollen Tubes. The Plant Cell tpc-

Geitmann A., Li Y.-Q., & Cresti M. (1996) The role of cytoskeleton and dictyosome activity in the pulsatory growth of Nicotiana tabacum and Petunia hybrida pollen tubes. Botanica Acta 109, 102-109.

Gu F. & Nielsen E. (2013) Targeting and Regulation of Cell Wall Synthesis During Tip Growth in Plants. Journal of Integrative Plant Biology 55, 835-846.

Hardin S.C., Winter H., & Huber S.C. (2004) Phosphorylation of the amino terminus of maize sucrose synthase in relation to membrane association and enzyme activity. Plant Physiol 134, 1427-1438.

Hedhly A. (2011) Sensitivity of flowering plant gametophytes to temperature fluctuations. Environmental and Experimental Botany 74, 9-16.

Heinlein M. & Starlinger P. (1989) Tissue- and cell-specific expression of the two sucrose synthase isoenzymes in developing maize kernels. Mol.Gen.Genet. 215, 441-446.

Hepler P.K. & Winship L.J. (2014) The pollen tube clear zone: Clues to the mechanism of polarized growth. Journal of Integrative Plant Biology

Kandasamy M.K. & Kristen U. (1989) Ultrastructural responses of tobacco pollen tubes to heat shock. 153, 104-110.

Kang S., Chen S., & Dai S. (2010) Proteomics characteristics of rice leaves in response to environmental factors. 5, 246-254.

Kaushal N., Awasthi R., Gupta K., Gaur P., Siddique K.H.M., & Nayyar H. (2013) Heat-stress-induced reproductive failures in chickpea (Cicer arietinum) are associated with impaired sucrose metabolism in leaves and anthers. 40, 1334-1349.

Kost B. (2008) Spatial control of Rho (Rac-Rop) signaling in tip-growing plant cells. Trends Cell Biol. 18, 119-127.

Ledesma N. & Sugiyama N. (2005) Pollen quality and performance in strawberry plants exposed to high-temperature stress. 130, 341-347.

Li Y.-Q., Faleri C., Geitmann A., Zhang H.Q., & Cresti M. (1995) Immunogold localization of arabinogalactan proteins, unesterified and esterified pectins in pollen grains and pollen tubes of Nicotiana tabacum L. Protoplasma 189, 26-36.

Li Z., Palmer W.M., Martin A.P., Wang R., Rainsford F., Jin Y., Patrick J.W., Yang Y., & Ruan Y.L. (2011) High invertase activity in tomato reproductive organs correlates with enhanced sucrose import into, and heat tolerance of, young fruit. Journal of Experimental Botany

Liu Z., Yuan Y.L., Liu S.Q., Yu X.N., & Rao L.Q. (2006) Screening for high-temperature tolerant cotton cultivars by testing in vitro pollen germination, pollen tube growth and boll retention. 48, 706-714.

Lorenzen J.H. & Lafta A.M. (1996) Effect of heat stress on enzymes that affect sucrose levels in potato shoots. 121, 1152-1156.

Lovy-Wheeler A., Wilsen K.L., Baskin T.I., & Hepler P.K. (2005) Enhanced fixation reveals the apical cortical fringe of actin filaments as a consistent feature of the pollen tube. Planta 221, 95-104.

Lu M.H., Gong Z.H., Chen R.G., Huang W., & Li D.W. (2009) High temperature stres on crop pollen: A review. 20, 1511-1516.

Magnard J.L., Vergne P., & Dumas C. (1996) Complexity and genetic variability of heat-shock protein expression in isolated maize microspores. Plant Physiology 111, 1085-1096.

Malerba M., Crosti P., & Cerana R. (2010a) Effect of heat stress on actin cytoskeleton and endoplasmic reticulum of tobacco BY-2 cultured cells and its inhibition by Co2+. 239, 23-30.

Malerba M., Crosti P., & Cerana R. (2010b) Effect of heat stress on actin cytoskeleton and endoplasmic reticulum of tobacco BY-2 cultured cells and its inhibition by Co2+. Protoplasma 239, 23-30.

Marrs K.A., Casey E.S., Capitant S.A., Bouchard R.A., Dietrich P.S., Mettler I.J., & Sinibaldi R.M. (1993) Characterization of two maize HSP90 heat shock protein genes: expression during heat shock, embryogenesis, and pollen development. Developmental genetics 14, 27-41.

Mascarenhas J.P. & Crone D.E. (1996) Pollen and the heat shock response. Sexual Plant Reproduction 9, 370-374.

McKenna S.T., Kunkel J.G., Bosch M., Rounds C.M., Vidali L., Winship L.J., & Hepler P.K. (2009) Exocytosis precedes and predicts the increase in growth in oscillating pollen tubes. Plant Cell 21, 3026-3040.

Mirzaei M., Soltani N., Sarhadi E., Pascovici D., Keighley T., Salekdeh G.H., Haynes P.A., & Atwell B.J. (2012) Shotgun proteomic analysis of long-distance drought signaling in rice roots. 11, 348-358.

Mittler R., Finka A., & Goloubinoff P. (2012) How do plants feel the heat? Trends in biochemical sciences 37, 118-125.

Mo Y., Liang G., Shi W., & Xie J. (2011) Metabolic responses of alfalfa (Medicago sativa L.) leaves to low and high temperature induced stresses. 10, 1117-1124.

Mohammadi P.P., Moieni A., Hiraga S., & Komatsu S. (2012) Organ-specific proteomic analysis of drought-stressed soybean seedlings. Journal of proteomics 75, 1906-1923.

Morell M.K., Li Z., & Rahman S. (2001) Starch biosynthesis in the small grained cereals: Wheat and barley. SPECIAL PUBLICATION-ROYAL SOCIETY OF CHEMISTRY 271, 129-137.

Müller J., Menzel D., & Šamaj J. (2007a) Cell-type-specific disruption and recovery of the cytoskeleton in Arabidopsis thaliana epidermal root cells upon heat shock stress. Protoplasma 230, 231-242.

Müller J., Menzel D., & Šamaj J. (2007b) Cell-type-specific disruption and recovery of the cytoskeleton in Arabidopsis thaliana epidermal root cells upon heat shock stress. Protoplasma 230, 231-242.

Parrotta L., Cresti M., & Cai G. (2013a) Accumulation and post-translational modifications of plant tubulins. Plant Biol. 16, 521-527.

Parrotta L., Cresti M., & Cai G. (2013b) Heat-shock protein 70 binds microtubules and interacts with kinesin in tobacco pollen tubes. 70, 522-537.

Patterson K.R., Ward S.M., Combs B., Voss K., Kanaan N.M., Morfini G., Brady S.T., Gamblin T.C., & Binder L.I. (2011) Heat shock protein 70 prevents both tau aggregation and the inhibitory effects of preexisting tau aggregates on fast axonal transport. Biochemistry 50, 10300-10310.

Persia D., Cai G., Del Casino C., Faleri C., Willemse M.T.M., & Cresti M. (2008) Sucrose synthase is associated with the cell wall of tobacco pollen tubes. Plant Physiol. 147, 1603-1618.

Petkova V., Nikolova V., Kalapchieva S.H., Stoeva V., Topalova E., & Angelova S. (2009) Physiological response and pollen viability of Pisum sativum genotypes under high temperature influence. 830, 665-671.

Pivovarova A.V., Chebotareva N.A., Chernik I.S., Gusev N.B., & Levitsky D.I. (2007) Small heat shock protein Hsp27 prevents heat-induced aggregation of F-actin by forming soluble complexes with denatured actin. FEBS J 274, 5937-5948.

Porter J.R. (2005) Rising temperatures are likely to reduce crop yields. Nature 436, 174-174.

Prasad P.V.V., Pisipati S.R., Mutava R.N., & Tuinstra M.R. (2008) Sensitivity of grain sorghum to high temperature stress during reproductive development. Crop Science 48, 1911-1917.

Pressman E., Harel D., Zamski E., Shaked R., Althan L., Rosenfeld K., & Firon N. (2006) The effect of high temperatures on the expression and activity of sucrose-cleaving enzymes during tomato (Lycopersicon esculentum) anther development. 81, 341-348.

Rounds C.M., Hepler P.K., & Winship L.J. (2014) The apical actin fringe contributes to localized cell wall deposition and polarized growth in the lily pollen tube. PLANT PHYSIOLOGY 166, 139-151.

Ruan Y.L., Jin Y., Yang Y.J., Li G.J., & Boyer J.S. (2010) Sugar input, metabolism, and signaling mediated by invertase: roles in development, yield potential, and response to drought and heat. Molecular Plant 3, 942-955.

Saini H.S. & Aspinall D. (1982) Abnormal sporogenesis in wheat (Triticum aestivum L.) induced by short periods of high temperature. Annals of Botany 49, 835-846.

Saini H.S., Sedgley M., & Aspinall D. (1983) Effect of heat stress during floral development on pollen tube growth and ovary anatomy in wheat (Triticum aestivum L.). 10, 137-144.

Sakurai T., Plata G., Rodr+¡guez-Zapata F., Seki M., Salcedo A.s., Toyoda A., Ishiwata A., Tohme J., Sakaki Y., & Shinozaki K. (2007) Sequencing analysis of 20,000 full-length cDNA clones from cassava reveals lineage specific expansions in gene families related to stress response. BMC Plant Biology 7, 66-

Salem M.A., Kakani V.G., Koti S., & Reddy K.R. (2007) Pollen-based screening of soybean genotypes for high temperatures. 47, 219-231.

Salnikov V.V., Grimson M.J., Seagull R.W., & Haigler C.H. (2003) Localization of sucrose synthase and callose in freeze-substituted secondary-wall-stage cotton fibers. Protoplasma 221, 175-184.

Sato S., Kamiyama M., Iwata T., Makita N., Furukawa H., & Ikeda H. (2006) Moderate increase of mean daily temperature adversely affects fruit set of Lycopersicon esculentum by disrupting specific physiological processes in male reproductive development. Annals of Botany 97, 731-738.

Serafini L., Hann J.B., Kültz D., & Tomanek L. (2011) The proteomic response of sea squirts (genus Ciona) to acute heat stress: A global perspective on the thermal stability of proteins. Comparative Biochemistry and Physiology Part D: Genomics and Proteomics 6, 322-334.

Silflow C.D., Sun X., Haas N.A., Foley J.W., & Lefebvre P.A. (2011) The Hsp70 and Hsp40 chaperones influence microtubule stability in Chlamydomonas. Genetics 189, 1249-1260.

Smertenko A., Dráber P., Viklický V., & Opatrný Z. (1997) Heat stress affects the organization of microtubules and cell division in Nicotiana tabacum cells. Plant, Cell & Environment 20, 1534-1542.

Snider J.L. & Oosterhuis D.M. (2011) How does timing, duration and severity of heat stress influence pollen-pistil interactions in angiosperms? 6, 12-15.

Snider J.L., Oosterhuis D.M., & Kawakami E.M. (2011a) Diurnal pollen tube growth rate is slowed by high temperature in field-grown Gossypium hirsutum pistils. 168, 441-448.

Snider J.L., Oosterhuis D.M., Loka D.A., & Kawakami E.M. (2011b) High temperature limits in vivo pollen tube growth rates by altering diurnal carbohydrate balance in field-grown Gossypium hirsutum pistils. 168, 1168-1175.

Staiger C.J., Poulter N.S., Henty J.L., Franklin-Tong V.E., & Blanchoin L. (2010) Regulation of actin dynamics by actin-binding proteins in pollen. J.Exp.Bot. 61, 1969-1986.

Vara Prasad P.V., Boote K.J., Hartwell Allen L., & Thomas J.M. (2003) Super-optimal temperatures are detrimental to peanut (Arachis hypogaea L.) reproductive processes and yield at both ambient and elevated carbon dioxide. Global Change Biology 9, 1775-1787.

Vara Prasad P.V., Craufurd P.Q., Kakani V.G., Wheeler T.R., & Boote K.J. (2001) Influence of high temperature during pre- and post-anthesis stages of floral development on fruit-set and pollen germination in peanut. 28, 233-240.

Wahid A., Gelani S., Ashraf M., & Foolad M.R. (2007) Heat tolerance in plants: an overview. Environmental and Experimental Botany 61, 199-223.

Wang J., Qian D., Fan T., Jia H., An L., & Xiang Y. (2012) Arabidopsis actin capping protein (AtCP) subunits have different expression patterns, and downregulation of AtCPB confers increased thermotolerance of Arabidopsis after heat shock stress. 193-194, 110-119.

Weis F., Moullintraffort L., Heichette C., Chretien D., & Garnier C. (2010) The 90-kDa heat shock protein Hsp90 protects tubulin against thermal denaturation. J Biol Chem. 285, 9525-9534.

Winter H., Huber J.L., & Huber S.C. (1998) Identification of sucrose synthase as an actin-binding protein. FEBS Lett. 430, 205-208.

Wollenweber B., Porter J.R., & Schellberg J. (2003) Lack of interaction between extreme high temperature events at vegetative and reproductive growth stages in wheat. Journal of Agronomy and Crop Science 189, 142-150.

Xu C. & Huang B. (2008) Root proteomic responses to heat stress in two Agrostis grass species contrasting in heat tolerance. 59, 4183-4194.

Yan S.H., Yin Y.P., Li W.Y., Li Y., Liang T.B., Wu Y.H., Geng Q.H., & Wang Z.L. (2008) Effect of high temperature after anthesis on starch formation of two wheat cultivars differing in heat tolerance. 28, 6138-6147.

Young L.W., Wilen R.W., & Bonham-Smith P.C. (2004) High temperature stress of Brassica napus during flowering reduces micro- and megagametophyte fertility, induces fruit abortion, and disrupts seed production. 55, 485-495.

Young T.E., Ling J., Geisler-Lee C.J., Tanguay R.L., Caldwell C., & Gallie D.R. (2001) Developmental and thermal regulation of the maize heat shock protein, HSP101. Plant Physiology 127, 777-791.

Zhang J., Jiang X., Li T., & Chang T. (2012) Effect of elevated temperature stress on the production and metabolism of photosynthate in tomato (Lycopersicon esculentum L.) leaves. 87, 293-298.

Zhang Y., He J., Lee D., & McCormick S. (2010) Interdependence of endomembrane trafficking and actin dynamics during polarized growth of Arabidopsis pollen tubes. PLANT PHYSIOLOGY 152, 2200-2210.

Zhao H., Dai T., Jiang D., & Cao W. (2008) Effects of High Temperature on Key Enzymes Involved in Starch and Protein Formation in Grains of Two Wheat Cultivars. Journal of Agronomy and Crop Science 194, 47-54.

Zhao H. & Ren H. (2006) Rop1Ps promote actin cytoskeleton dynamics and control the tip growth of lily pollen tube. Sexual Plant Reproduction 19, 83-91.

Zheng Y., Anderson S., Zhang Y., & Garavito R.M. (2011) The Structure of Sucrose Synthase-1 from Arabidopsis thaliana and Its Functional Implications. Journal of Biological Chemistry 286, 36108-36118.

Zinn K.E., Tunc-Ozdemir M., & Harper J.F. (2010) Temperature stress and plant sexual reproduction: Uncovering the weakest links. 61, 1959-1968.

FIGURE LEGENDS

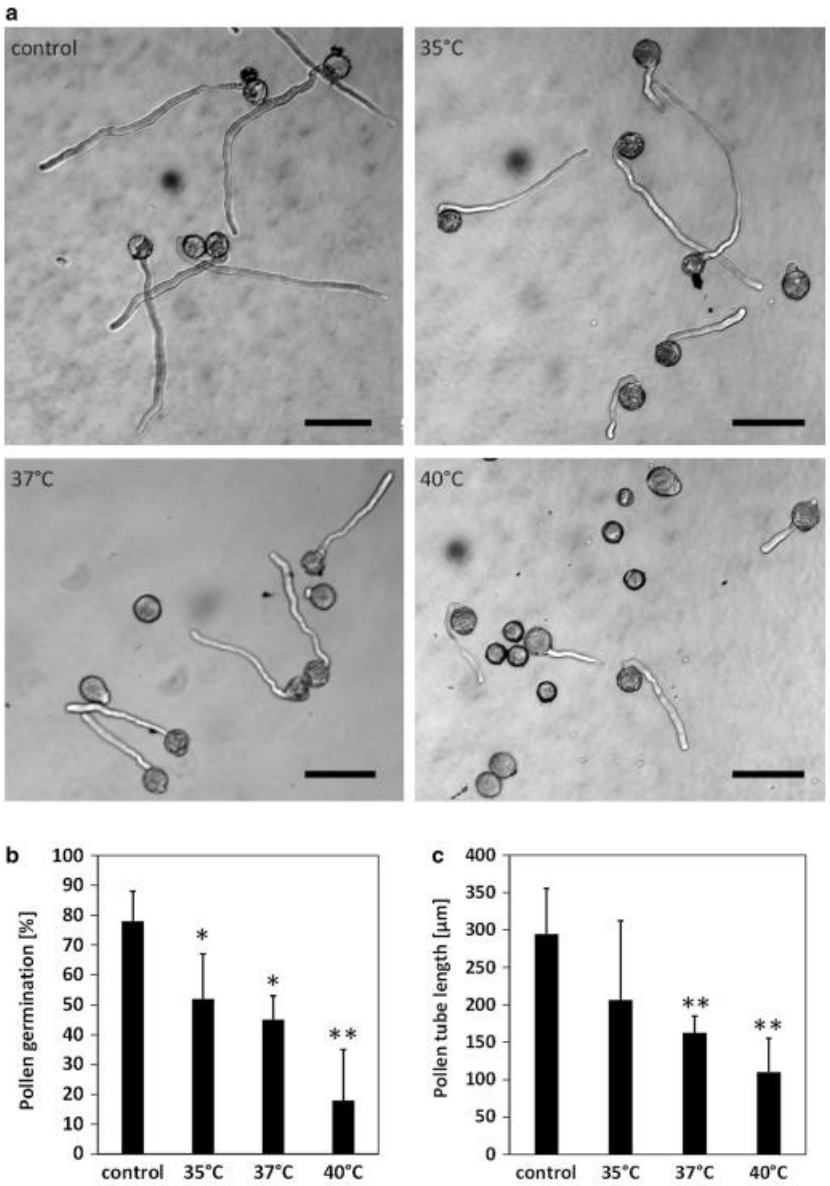

Figure 1. Germination rate and tube length of heat-stressed pollen grains. (A) Representative microscopy images of pollen grains germinated after incubation at room temperature (control), at 35, 37 and 40 °C. Bars: 100-150 µm. (B) Germination rate (%) of pollen grains after incubation at room temperature (control), 35, 37 and 40°C. Asterisks indicate statistically-significant differences (one asterisk for $p<0.05$, two asterisks for $p<0.01$). (C) Length of pollen tubes germinating from pollen grains incubated at room temperature (control), 35, 37 and 40°C. Asterisks indicate statistically-significant differences (one asterisk for $p<0.05$, two asterisks for $p<0.01$).

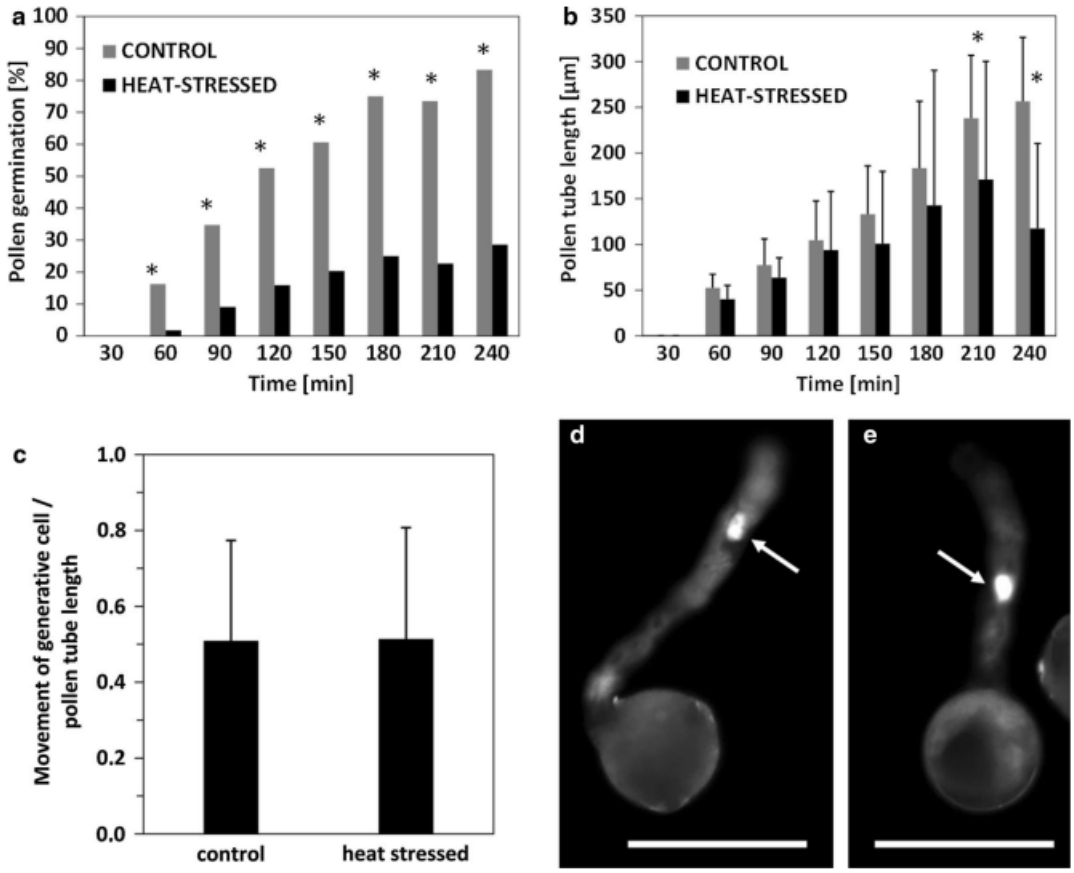

Fig. 2 Analysis of heat stress on germination, tube extension rate and movement of generative cells. a The germination rate of heat-stressed pollen grains is greatly affected soon after the first hour of germination and the effect increased up to 4 h. b The pollen tube elongation rate was less affected suggesting that heat stress critically affected the germination step. Asterisks indicate statistically significant differences between control and heat-stressed samples for P\0.05. c The distance traveled by generative cells was measured and normalized to the pollen tube length. When pollen tubes germinated for at least 4 h, generative cells moved into pollen tubes and covered a similar distance in comparison to control pollen tubes. Error bars are standard deviation. No statistically significant differences were found for P\0.05. d Representative image of a control pollen tube. e Representative image of a heat-stressed pollen tube. Bars 50 lm. Arrows indicate the generative cells.

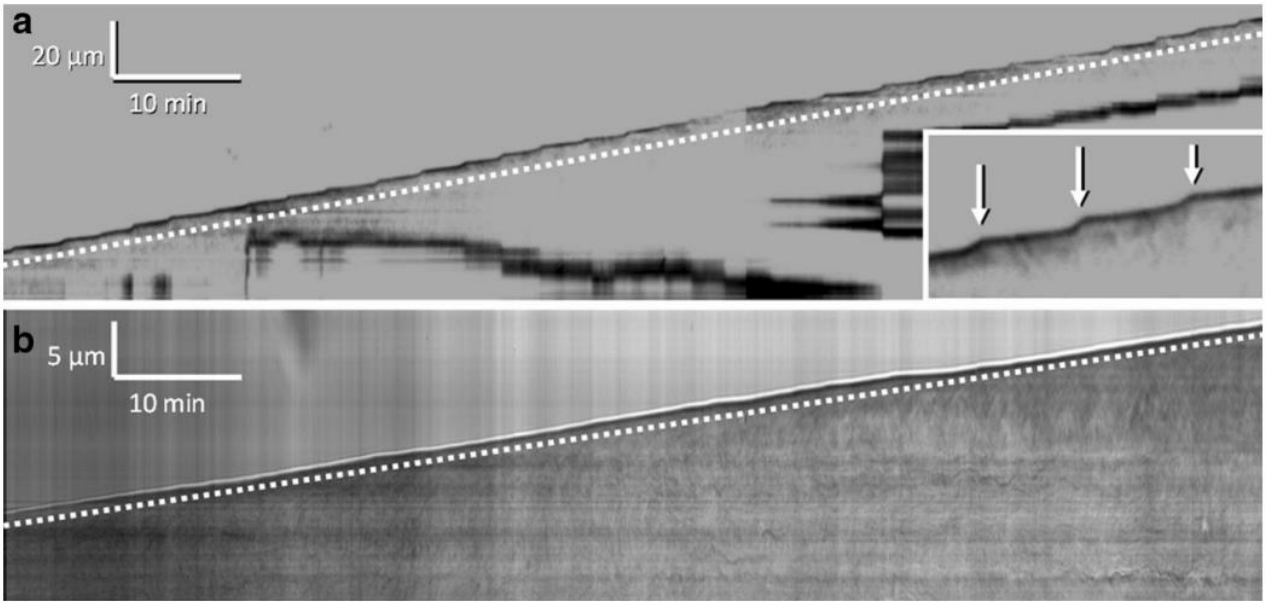

Figure 3. Kymograph analysis of pollen tubes. (A) A pollen tube germinated from pollen grain incubated at room temperature. The dotted white line remarks the linearity of the growth profile. Inset: the growth profile is a succession of slow growth periods interspersed by peaks of fast growth (arrows). Bars for time and length are shown in the top left corner. (B) Kymograph analysis of a pollen tube germinated from pollen grain treated at 40°C. Note the different speed as represented by the different length scale. Although the growth speed is different, growth is still linear but oscillations between slow and fast growth phases are lost. Bars for time and length are shown in the top left corner. In both A and B cases, the profile shown is representative of different pollen tubes.

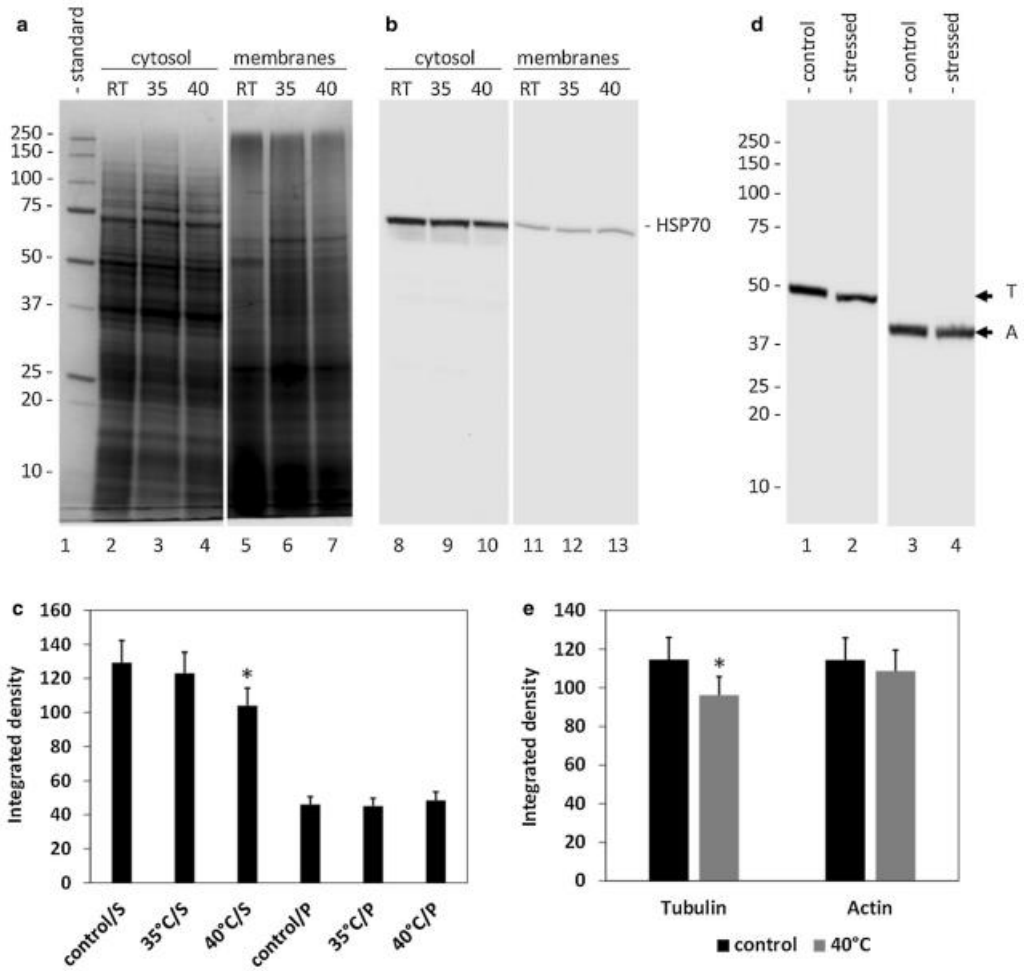

Figure 4. Immunoblot analysis of HSP70, actin and tubulin. (A) Electrophoresis of cytosolic (lanes 2-3-4) and membrane (lanes 5-6-7) proteins extracted from pollen tubes germinated from untreated pollen grains (room temperature, RT) or pollen grains stressed at 35°C or 40°C. Lane 1: molecular mass standards. Equivalent amount of proteins (30 µg) are loaded in each lane. (B) Immunoblot with the antibody to HSP70 on identical samples. (C) Immunoblot with tubulin antibody (left panel) and actin antibody (right panel) on cytosolic proteins extracted from control pollen tubes (lane 1, 3) and pollen tubes grown from pollen grains heat-stressed at 40°C (lanes 2, 4). (D) Relative quantitation of three different immunoblots against HSP70 on cytosolic (S) and membrane proteins (P) from pollen tubes after control and heat-stress treatment of pollen grains at 35 and 40°C. Asterisk indicates statistically-significant differences for $p<0.05$. (E) Relative quantitation of three different immunoblots on cytosolic tubulin and actin from pollen tubes grown after no treatment (control) and heat treatment of pollen grains at 40°C. Asterisk indicates statistically-significant differences for $p<0.05$.

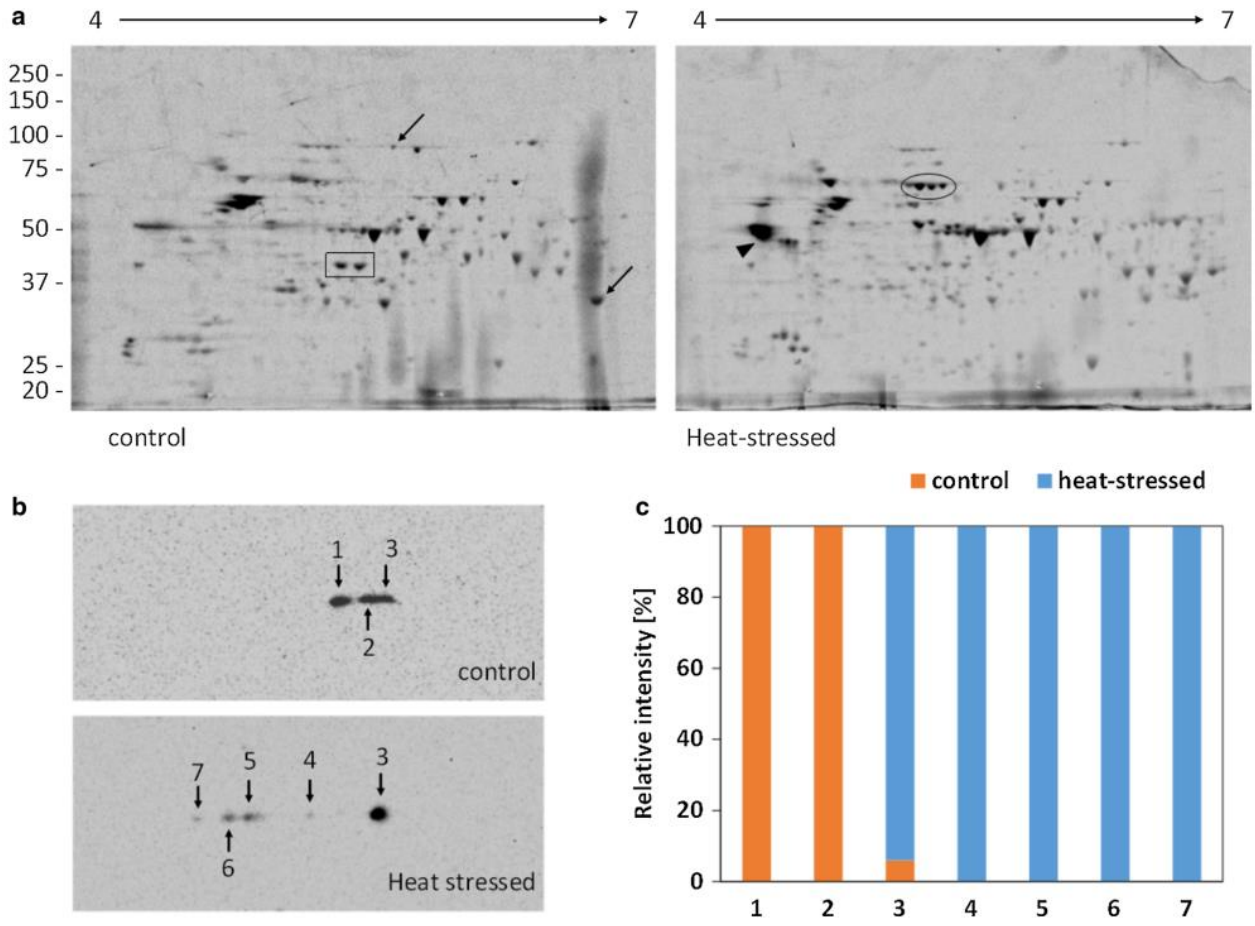

Figure 5. Analysis of tubulin by bidimensional electrophoresis and blot. (A) Representative 2-D gels of pollen tubes germinated from pollen grains incubated at either room temperature (control, left gel) or 40°C (heat-stressed, right gel). Arrows indicate spots found only in controls while arrowheads show spots typical of treated samples; circles highlight spots overexpressed in heat-stressed samples while rectangles mark spots over-expressed in control pollen. Molecular mass standards are indicated on the left side, while the pH range is in the top. Equivalent protein contents (200 µg) were loaded. (B) 2-D immunoblot of tubulin on pollen tube extracts after incubation of pollen grains at room temperature (control, top panel) and at 40°C (heat-stressed, bottom panel). Tubulin spots are numbered consecutively and spots with identical position have the same number. Only the blot region containing spots is reported. (C) Average of relative percentage of three independent tubulin blots in the two experimental conditions. Gray bars are spots present in controls while black bars indicate tubulin spots present in heat-stressed samples.

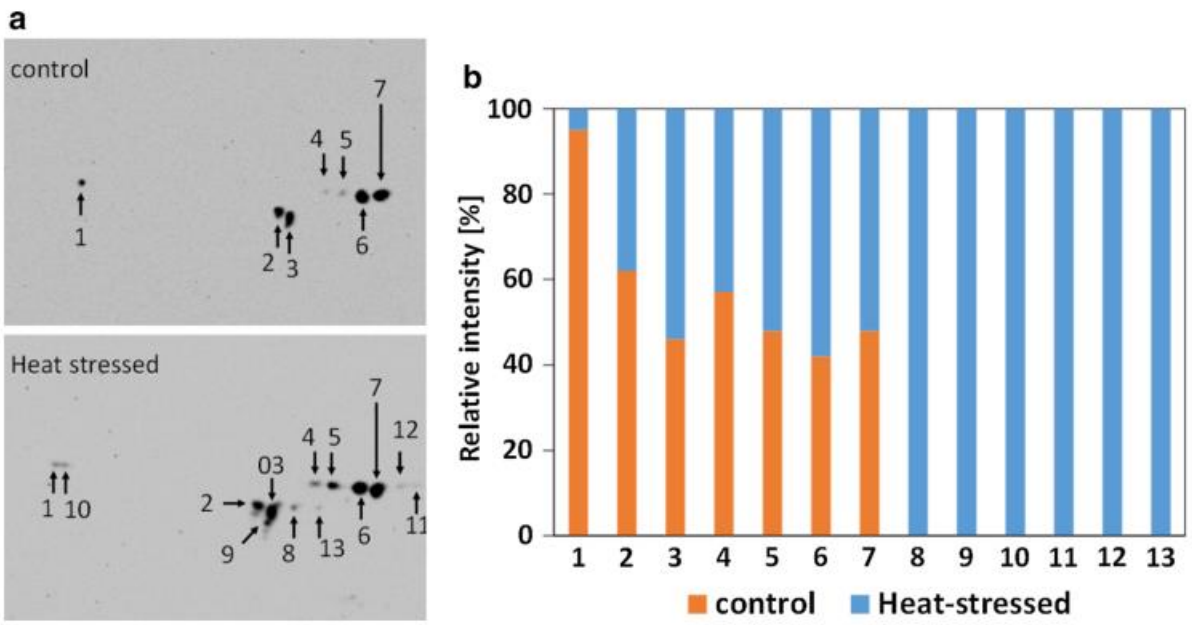

Figure 6. Bidimensional electrophoresis and immunoblot of actin. (A) Immunoblot analysis of actin in pollen tubes from control (top) and heat-stressed (bottom) pollen grains. Spots are numbered consecutively. Spots with identical position have the same number in both blots. Only the blot region with spots is reported. (B) Average of relative percentage of actin spots from three different 2-D blots; gray bars indicate spots present in control samples while black bars indicate spots present in heat-stressed samples. Spot number is the same as in panel A.

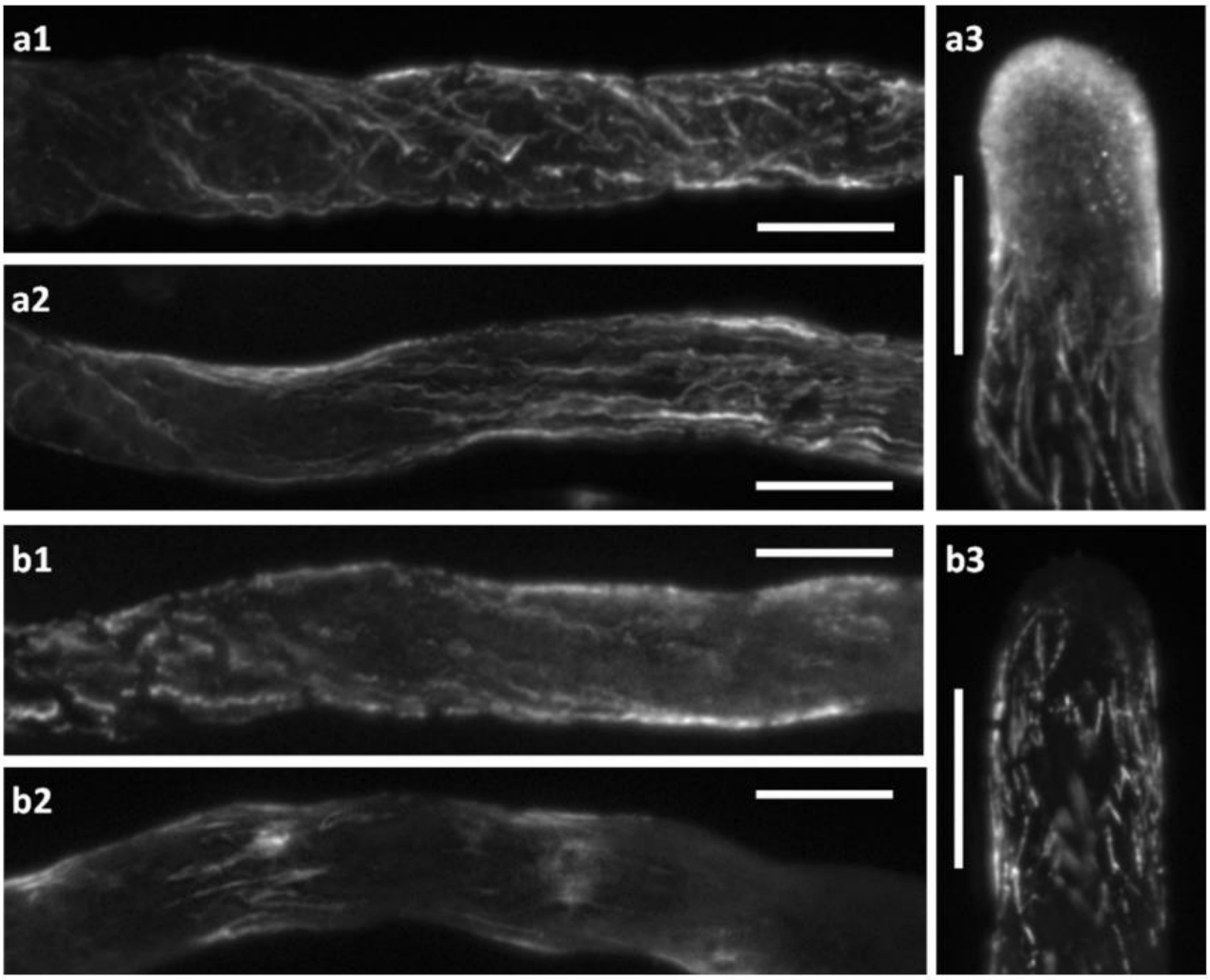

Figure 7. Immunofluorescence of tubulin. (A1-A2) Immunolocalization of tubulin in control pollen tubes. Images are Z-projects of several 500 nm-sections obtained with the Apotome module. Bar: 10 µm. (A3) Detail of the apical dome of a pollen tube. Image is a Z-project of 10 Apotome sections of 1 µm each. Bar: 10 µm. (B1-B2) Distribution of tubulin in pollen tubes germinated from 40°C heat-stressed pollen grains. Images are Z-projects of several 500 nm-sections obtained with the Apotome module. Bar: 10 µm. (B3) Detail of a pollen tube apex from heat-stressed pollen grain. Fifteen Apotome sections were used to reconstruct the Z-project. Bar: 10 µm.

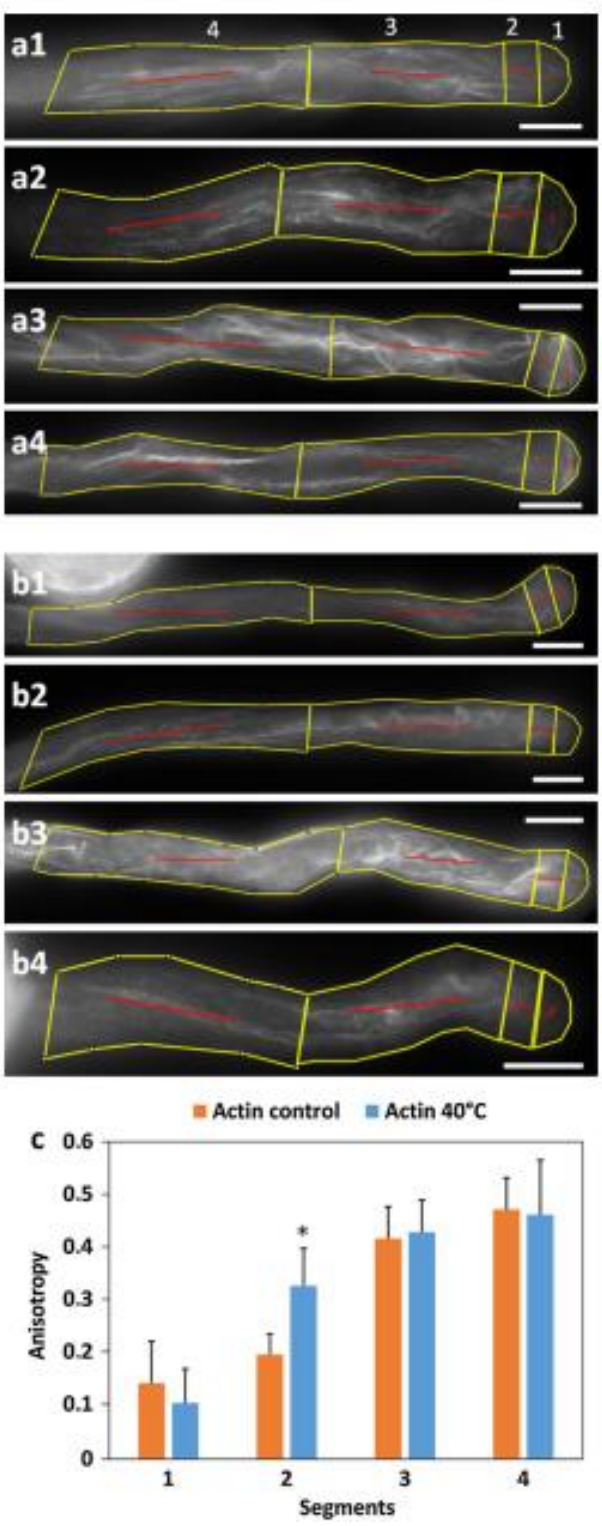

Figure 8. Analysis of actin filament orientation by FibrilTool. Pollen tubes were arbitrarily subdivided into four segments: the hemispherical dome (segment 1), the next 5-µm subapical segment (n. 2), the next 30-µm segment (n. 3) and a final 30-µm segment (n. 4). The segment border is shown in yellow while the anisotropy of fiber arrays is indicated by red lines. (A1 to A4) Pollen tubes from pollen grains incubated at room temperature. (B1 to B4) Pollen tubes from pollen grains heat-stressed at 40°C. All images are Z-projects of several Apotome sections of identical thickness. Bars: 10 µm. (C) Statistical analysis of anisotropy from both control (orange bars) and heat-stressed (blue bars) samples in the four segments. Asterisk indicates statistically-significant differences for $p<0.05$.

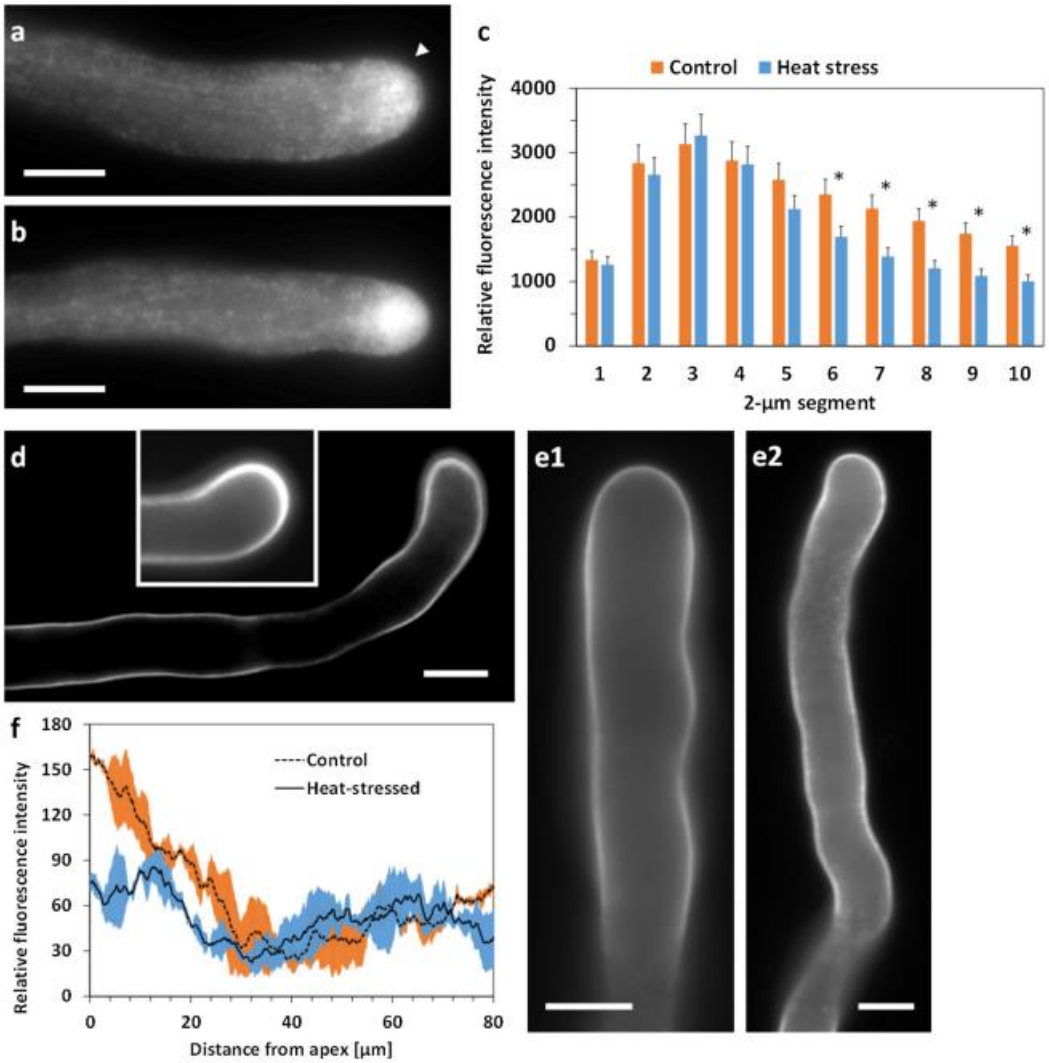

Figure 9. Distribution of Rab11b-labelled vesicles and PI-labelled cell wall in control and heat-stressed samples. (A) Representative pollen tube showing Rab11b-labelled vesicles after incubation at room temperature. (B) Representative pollen tube from 40°C heat-stressed pollen grain displaying Rab11b-labelled vesicles. (C) Fluorescence intensity in control pollen tubes and in pollen tubes after heat stress of pollen grains as measured for every 2-µm segments (segment 1 is the closest to the tip). All measures were done in 1-µm Apotome sections in central focal planes. Bars: 10 µm. (D, with inset) Labelling of newly secreted cell wall by PI in control pollen tubes. Bar: 10 µm. (E1-E2) Pollen tubes from heat-stressed pollen grains as stained by PI. Bar: 10 µm. Images in D and E are central focal planes. (F) Measurement of fluorescence intensity on the cell border of untreated (gray line) and heat-stressed pollen tubes (black line) from the apex down to 80 µm.

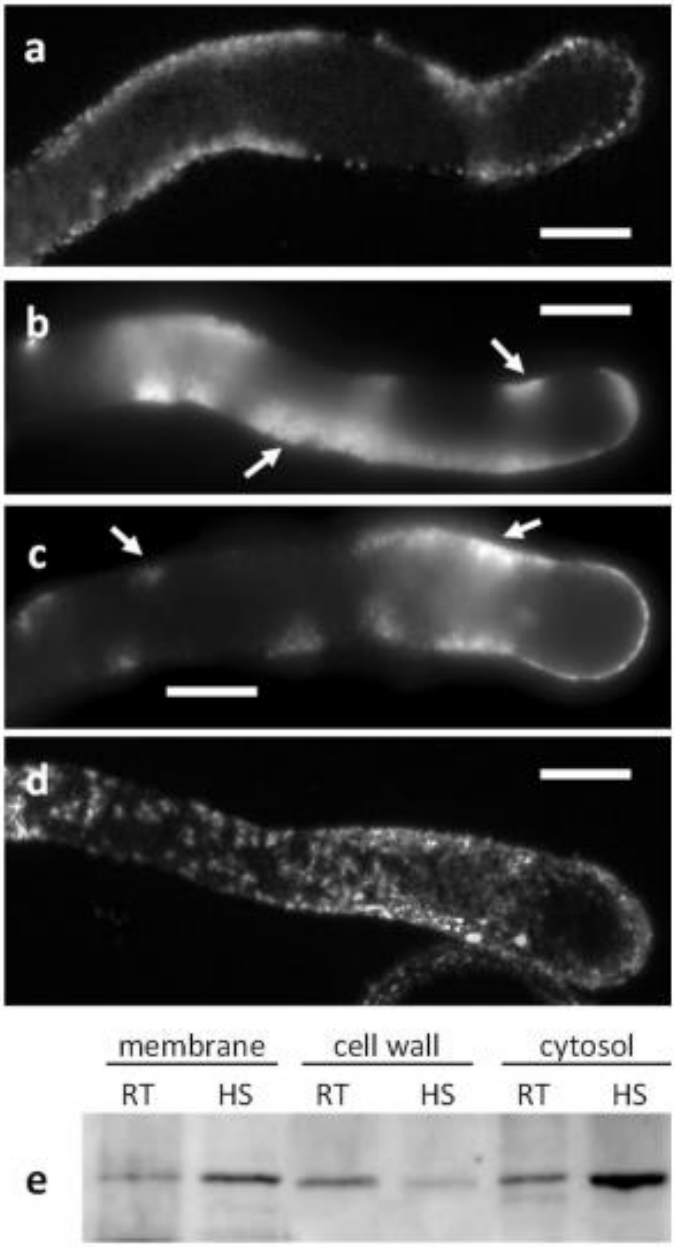

Figure 10. Immunocytochemical and immunochemical analysis of sucrose synthase. (A) Distribution of sucrose synthase in pollen tubes germinated from control pollen grains. (B, C, D) Localization of sucrose synthase in pollen tubes germinated from 40°C heat-stressed pollen grains. Arrows indicate consistent accumulations of sucrose synthase in heat-treated samples. Bars: 10 µm. (E) Immunoblot analysis of sucrose synthase in different protein fractions (cytosol, membranes and cell wall) from pollen tubes germinated after incubation of pollen grains at room temperature (RT) or 40°C (HS). Identical protein contents were loaded in each lane.

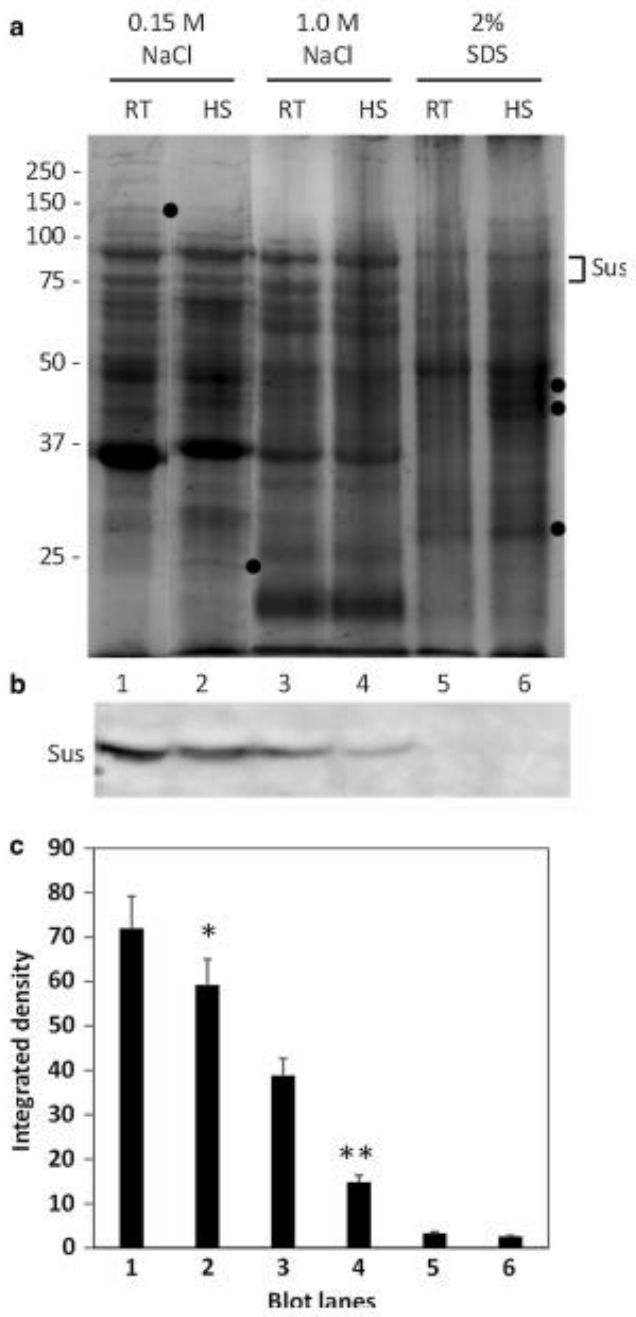

Figure 11. Characterization of cell wall proteins from control and heat-stressed samples. (A) Electrophoretic analysis of cell wall proteins extracted by sequential treatment with 0.15 M NaCl, 1 M NaCl and 2% SDS. RT (room temperature): lanes from control samples. HS, lanes from heat-stressed samples. Molecular mass are indicated on the left. Identical protein contents were loaded for each extraction treatment. Dots indicated bands that differ significantly from the corresponding sample. (B) Immunoblot against sucrose synthase on the same fractions as in A. (C) Relative quantitation of sucrose synthase from three different blots. Asterisks indicate statistically-significant differences (one asterisk for $p<0.05$, two asterisks for $p<0.01$).

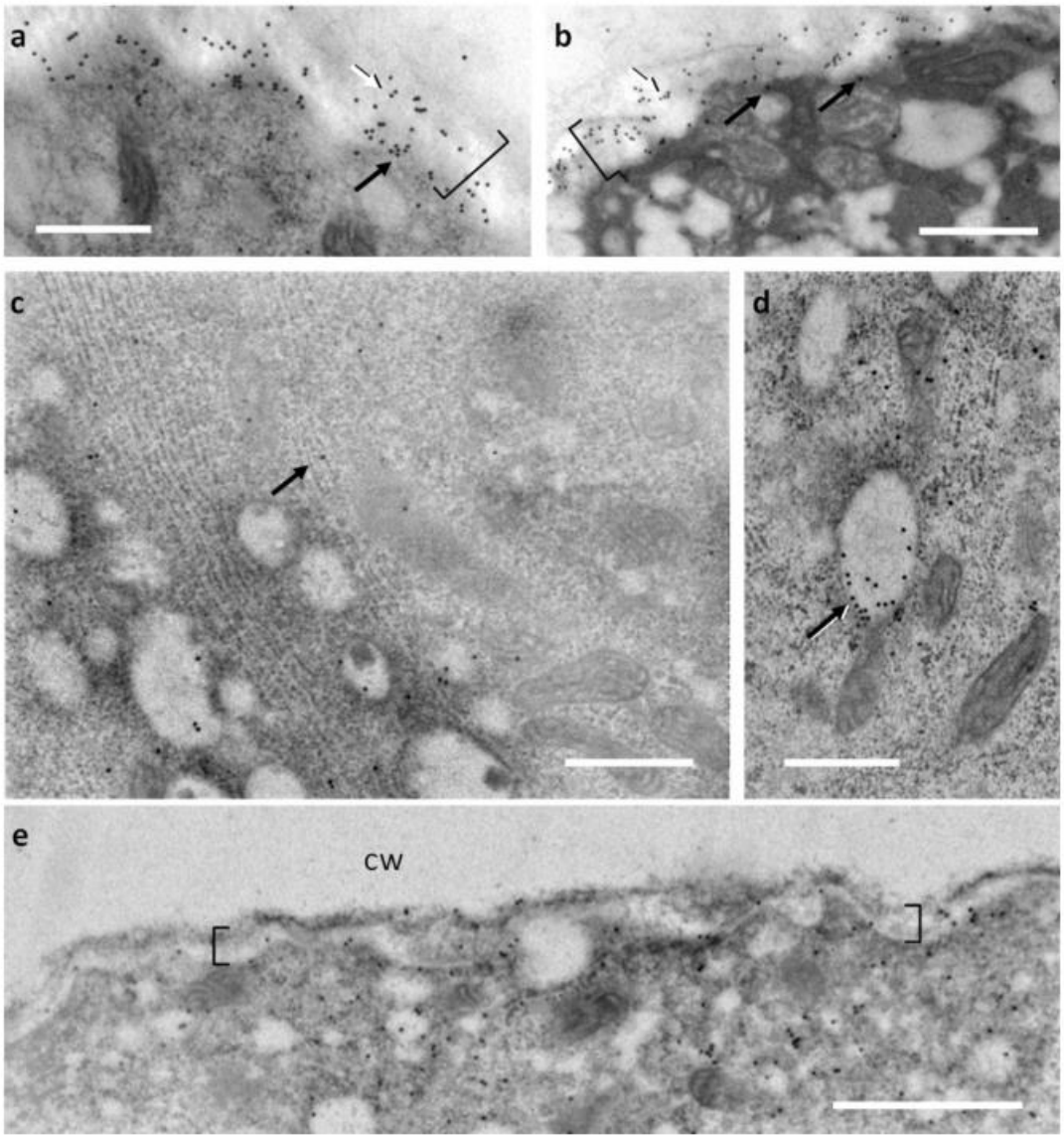

Figure 12. Immunogold labeling of sucrose synthase in control and heat-stressed samples. (A-B) Distribution of sucrose synthase in the subapical region of control pollen tubes. Black arrows indicate sucrose synthase in association with the plasma membrane while white arrows show sucrose synthase in the cell wall. Square bracket indicates approximately the cell wall thickness. Bar in A: 500 nm; bar in B: 1000 nm. (C-E) Localization of sucrose synthase in pollen tubes germinated from pollen grains heat-stressed at 40°C. Gold particles are found in association with the endoplasmic reticulum (C, arrow) and with vesicular structures (D, arrow). A very low number of gold particles were found in association with the plasma membrane or the cell wall (E, cw). Square bracket indicates the cell wall thickness. Bar in C and E: 1000 nm. Bar in D: 500 nm.